Targeting and cell uptake monitoring of biologics for cancer

Nora Osmonen

Master's Thesis in Pharmacy

Pharmacy, Faculty of Science and Engineering

Åbo Akademi University

Turku, Finland

2023

Supervisors:

Tapani Viitala

Åbo Akademi University

Oliver Koivisto

Åbo Akademi University

ABSTRACT

Master's Thesis, Åbo Akademi University, Turku, Finland

Faculty: Faculty of Science and Technology Subject: Pharmacy

Author: Nora Osmonen

Title of the work: Targeting and cell uptake monitoring of biologics for cancer

Supervisors: Tapani Viitala, Åbo Akademi
Oliver Koivisto, Åbo Akademi

Abstract

The surface plasmon resonance technique has recently been widely utilized in a wide range of biotechnological and microbiological applications. This masters' thesis project is a collaboration between Åbo Akademi University and Orion Pharma. The aim of the project was to monitor the interactions between human ovarian adenocarcinoma cells (SK-OV-3), two different protein-based antibody drugs, and a negative control (IgG). The interactions were measured with a surface plasmon resonance instrument, and complementary measurements and controls were performed with confocal microscopy and LigandTracer instrument. Based on the measured signals, the surface plasmon resonance technique was assessed and elucidated to study whether the technique could be utilized for differentiating between the surface interaction and internalization of protein-based drugs.

The results from the surface plasmon resonance measurements show that the method did not give replicable results. The concentration differences are clearly seen in short injections (20 minutes), but not in longer injections (4 hours). The results from the LigandTracer measurements show that trastuzumab and cetuximab have stronger interactions with the SK-OV-3 cells than IgG. Confocal microscopy pictures reveal that trastuzumab has primarily surface interactions with the cells and cetuximab has fewer surface interactions and is primarily taken up by the cells. IgG has overall very weak interactions with the cells.

Keywords: Surface plasmon resonance, surface interaction, internalization, biological cancer drug, LigandTracer, confocal microscopy, adenocarcinoma cells

Additional information

Date: 05/2023 Number of pages: 57

ABSTRAKT

Pro gradu-avhandling, Åbo Akademi, Åbo, Finland
Fakultet: Naturvetenskaper och teknik Läroämne: Farmaci
Författare: Nora Osmonen
Arbetets titel: Växelverkan och cellupptagningsprocess av biologiska läkemedel för cancer
Handledare: Tapani Viitala, Åbo Akademi Oliver Koivisto, Åbo Akademi
Abstrakt Tekniken ytplasmonresonans (SPR) har nyligen använts i stor utsträckning för olika typer av bioteknologiska och mikrobiologiska tillämpningar. Det här examensarbetet är ett samarbete mellan Åbo Akademi och Orion Pharma. Syftet med projektet var att mäta interaktioner och växelverkan mellan humana adenokarcinomaceller (SK-OV-3), två olika proteinbaserade antikroppsläkemedel, samt en negativ kontroll (IgG). Interaktionerna mättes med ett ytplasmonresonans instrument och kompletterande mätningar och kontroller utfördes med konfokalmikroskopi och LigandTracer-instrument. Baserat på de uppmätta signalerna bedömde och belyste vi om tekniken ytplasmonresonans kunde användas för att upptäcka skillnaden mellan ytinteraktionen och internaliseringen av de proteinbaserade läkemedlen. Resultaten från ytplasmonresonansmätningarna visar att metoden inte gav replikerbara resultat. Koncentrationsskillnaderna syns tydligt med korta injektioner (20 minuter), men inte med längre injektioner (4 timmar). Resultaten från LigandTracer-mätningarna visar att trastuzumab och cetuximab har starkare interaktioner med SK-OV-3-cellerna än IgG. Konfokalmikroskopibilder avslöjar att trastuzumab har främst ytinteraktioner med cellerna och cetuximab har mindre ytinteraktioner men tas primärt upp av cellerna. IgG har generellt sett mycket svaga interaktioner med cellerna.
Nyckelord: Ytplasmonresonans, ytinteraktion, internalisering, biologiska cancerläkemedel, konfokalmikroskopi, LigandTracer, adenokarcinomacell
Övriga uppgifter
Datum: 05/2023 Antal sidor: 57

ABSTRAKTI

Pro gradu -tutkielma, Åbo Akademi, Turku, Suomi

Tiedekunta: Luonnontieteet ja tekniikka Oppiaine: Farmasia

Kirjoittaja: Nora Osmonen

Tutkielman aihe: Biologisten syöpälääkkeiden soluun kohdistus ja soluun sisäänoton seuranta

Ohjaajat: Tapani Viitala, Åbo Akademi
Oliver Koivisto, Åbo Akademi

Abstrakti

Pintaplasmoniresonanssi -tekniikkaa on viime aikoina käytetty laajasti erilaisissa bioteknologisissa ja mikrobiologisissa sovelluksissa. Tämä pro graduprojekti on toteutettu yhteistyönä Åbo Akademin ja Orion Pharman välillä. Projektin tavoitteena oli seurata ihmisen adenokarsinoomasolujen (SK-OV-3), kahden eri proteiinipohjaisen vasta-aineläkkeen ja negatiivisen kontrollin (IgG) välisiä vuorovaikutuksia. Vuorovaikutuksia mitattiin pintaplasmoniresonanssilaitteella ja tarkentavat mittaukset ja kontrollit suoritettiin käyttäen konfokaalimikroskopiaa ja LigandTracer-laittetta. Mitattujen signaalien perusteella arvioimme ja selvitimme, voidaanko pintaplasmoniresonanssitekniikkaa käyttää proteiinipohjaisten lääkkeiden solujen pintainteraktioiden ja -sisäänoton välisen eron havaitsemiseen.

Pintaplasmoniresonanssimittausten tulokset osoittavat, että kyseinen menetelmä ei antanut toistokelpoisia tuloksia. Konsentraatioerot näkyvät selvästi lyhyissä injektioissa (20 minuuttia), mutta eivät pidemmissä injektioissa (4 tuntia). LigandTracer-mittausten tulokset osoittavat, että trastutsumabilla ja setuksimabilla on voimakkaampi vuorovaikutus SK-OV-3-solujen kanssa kuin IgG:llä. Konfokaalimikroskooppikuvat paljastavat, että trastutsumabilla on pääasiassa pintavuorovaikutuksia solujen kanssa ja setuksimabilla on vähemmän pintavuorovaikutuksia, mutta se päätyy pääasiassa solujen sisään. IgG:llä on erittäin heikkoja vuorovaikutuksia solujen kanssa.

Avainsanat: Pintaplasmoniresonanssi, pintainteraktio, soluun sisäänotto, biologiset syöpälääkkeet, konfokaalimikroskopia, LigandTracer, adenokarsinoomasolut

Lisäinformaatio

Päiväys: 05/ 2023 Sivumäärä: 57

TABLE OF CONTENTS

LIST OF ABBREVIATIONS

1xPBS	Phosphate buffered saline diluted to 1:10 with MilliQ water
FBS	Fetal bovine serum, used to provide the essential growth factors for the cells (ThermoFisher b), 2023)
Hepes	Used as an ingredient in the cell culture medium to achieve extra buffering capacity for the cells (ThermoFisher b), 2023)
MilliQ	Ultrapure water, which is filtrated and deionized, produced by the reverse osmosis water purification process (The emerging sciences, 2022)
NA	Numerical aperture, a factor used in light microscopy
PBS	Phosphate buffered saline is a salt solution containing water and essential inorganic ions for the cells. Used to e.g., washing of the cell cultures (ThermoFisher b), 2023)
Phage (P)	Generation of cell line
SK-OV-3	Human adenocarcinoma cell line
SPR	Surface plasmon resonance
SPR buffer	Cell medium containing 25mM hepes in 15 ml of the solution
Trypsin-	Used to detach the adherent cell cultures, e.g., when splitting the culture
Edta	(ThermoFisher b), 2023)
WT	Weight

1. INTRODUCTION

This project is a collaboration between Orion Pharma and Åbo Akademi University. Orion Pharma is the financier of this project and is assigned to purchase and deliver all the materials needed in the laboratory work.

The objective of the project is to monitor the interactions between EGFR- and HER_2- targeted biological antibodies and SK-OV-3- cells. The interactions between the antibodies and cells are studied with the surface plasmon resonance technique. With this technique, the cell interactions can be measured in real time without any markers, such as fluorescent substances.

The surface plasmon resonance technique is an optical biosensor, which can detect the kinetics of different types of macromolecular interactions as well as high- and low-affinity small molecular interactions. This technique has recently been used, for example, for applications in microbiology, virology, protein-, membrane-, cell-, and nucleic acid interaction measurements (Pattnaik, 2005). In Finland, the technique has been used, for example, by Suutari et al. for label-free monitoring of nanoparticle cell uptake, and label-free analysis with multiple parameters to separate G-protein coupled receptor signaling pathways (Suutari et al., 2016) (Suutari et al., 2020).

Confocal microscopy was used as a complementary technique to verify the results obtained from the SPR measurements. The method is based on producing a point source of light which generates a complete image of the sample by moving the spot over the sample. Confocal microscopy provides 3D reconstructions of the samples with a high resolution and has an ability to image deep into the tissues. (Elliott, 2020)

LigandTracer is another complementary technique that was used in this project. With this technique, it is possible to distinguish the affinity and the kinetics between the ligand and the receptor (LigandTracer, 2023). The association and dissociation phases between the cells and the ligands were measured in real-time by utilizing fluorescent substances.

2. LITERATURE REVIEW

2.1. Surface plasmon resonance

2.1.1. History and applications

Surface plasmon resonance (SPR) is a label-free technique that can be utilized in several different biomolecular fields. This detection method enables measuring of the interactions between ligands and their target(s) in real-time with a high sensitivity. Due to the label-free detection method, also sensitive targets and ligands can be used, enabling the applications of, for example, sensitive biomolecules and clinical analysis of their interactions. (Nguyen et al., 2015)

The surface plasmon resonance technique was introduced at the beginning of the 1990s. However, the last two decades have been the most promising to witness the breakthrough of the technique in, for example, health and biological sciences (Puiu and Bala, 2016). It has been shown lately that the SPR method is suitable for analyzing, for example, multiple different biomolecular interactions. It is a very powerful technology to determine and investigate the specificity, affinity and kinetic rates of the target(s) and ligand(s) (Nguyen et al., 2015). Additionally, SPR is also used in environmental and industrial areas, for example, to monitor liquid and gas phase mixtures, to measure organic vapors and salinity, and to measure the mixing dynamics (Masson et al., 2004; Nguyen et al., 2015).

The technique has been used to analyze the interactions between different biological macromolecules, such as protein-protein, protein-DNA, enzyme-substrate, enzyme-inhibitor, receptor-drug, lipid membrane-protein, protein-polysaccharide, cell-protein, virus-protein, antibody-antigen, and other interaction reactions. The SPR technique can be utilized, for example, in disease diagnostics, drug discovery, foodborne pathogen detection, epitope mapping, hybridization kinetics, enzymatic modifications, and monitoring of interactions between metallic- and carbon-based nanomaterials and their targets, such as antibodies. The

SPR technique has also been widely used as a complementary method to verify the conformational changes in, for example, protein-small molecular interactions. (Nguyen et al., 2015). Figure 1 presents the principle of the SPR technique.

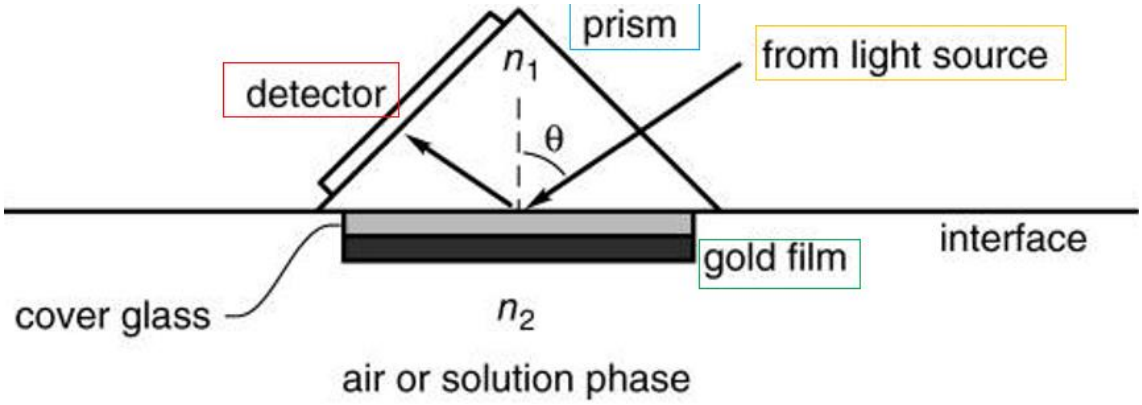

Figure 1. A simplified overall picture of the SPR technique (lino-Biotech, 2021). The light source generates a beam of light which is directed through a prism. The light is reflected from the surface of a gold-covered glass sensor and recorded by the detector.

2.1.2. The measuring principle

Surface plasmon resonance is an optical technique, that measures the changes in the refractive index in close vicinity of a thin sensor chip covered with a metal layer. The metal layer has band electrons that can resonate with the incident light at a certain wavelength (gold, silver, copper, indium or aluminum) (Nguyen et al., 2015; SPR-Pages, 2022). Gold sensors are usually preferred, because gold is chemically inert to liquids commonly used in biological applications. Gold is also resistant to oxidation and is therefore the most potential option to give an adequate SPR signal. A picture of the gold sensor is shown in Figure 2.

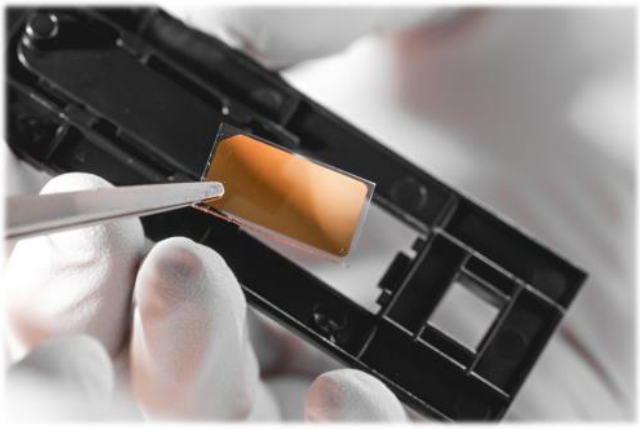

Figure 2. Bionavis' gold sensor used in SPR measurements (Bionavis, 2021). The sensor consists of glass, which is covered with a gold layer.

The thickness of the gold layer should be approximately 50 nm to avoid too shallow or too broad dips in the reflective light (SPR-Pages, 2022). A typical composition of a gold-coated biosensor is presented in Figure 3.

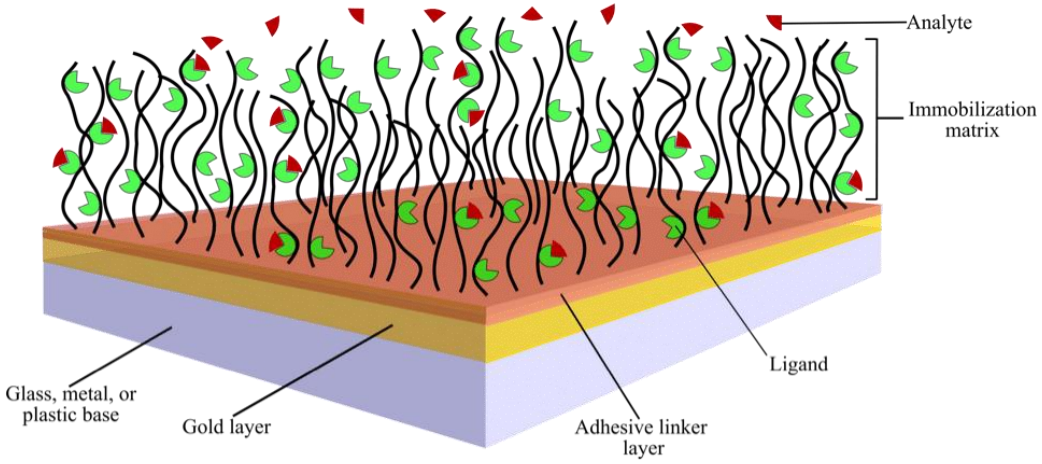

Figure 3. A typical composition of a gold biosensor used for SPR measurements (bitesizebio, 2017). The base of the sensor is covered with a gold surface, and sometimes also with an adhesive linker layer. Ligands are deposited on the sensor surface and are therefore exposed to analytes.

Total internal reflection (TIR) occurs because of a beam from the light source hits the thin film of a noble metal and is then bent towards the interface of two substances. The light passes from a denser medium to a less dense medium. By changing the incidence angle, the out-coming angle is changed until the TIR is reached, that is, when all the incoming light is reflected. With a certain energy of the photon in the electrical field, the interactions between

the photon and the free electrons on the golden surface can be formed. The energy of the light is, therefore, transferred to the electrons when the energy level of the photons is right. The photons are then converted to plasmons, which can be noticed as a gap in the reflected light intensity. (SPR-Pages, 2022). A schematic picture of the technique is presented in Figure 4.

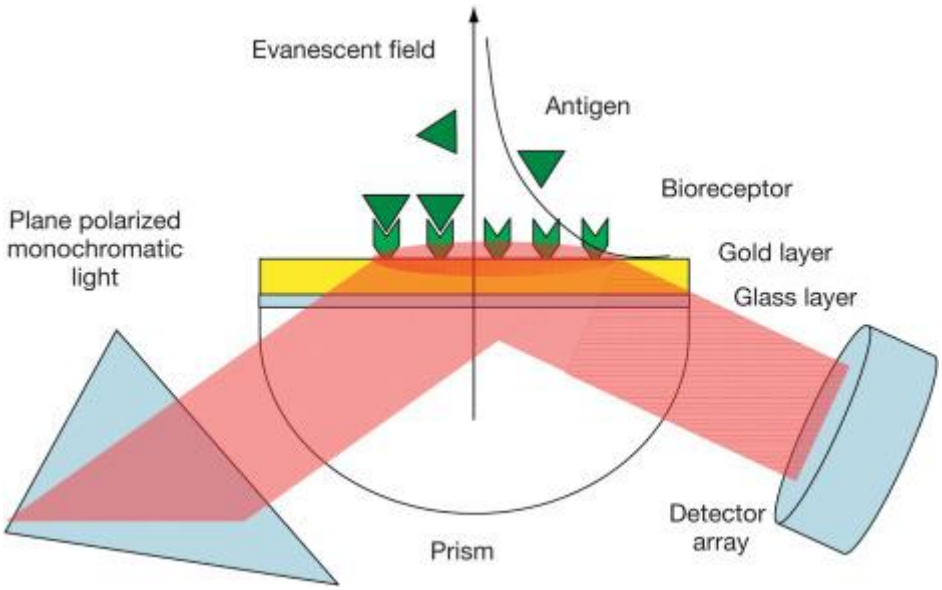

Figure 4. A schematic picture of the SPR technique utilizing a bioreceptor (Griffin et al., 2019). Antigens bind to the bioreceptors deposited on a gold layer. The interactions are detected by sensing the differences in the reflected p-polarized light by the detector.

Surface plasmon resonance phenomenon occurs under certain optical premises when a photon of plane-polarized light hits a metal surface (SPR-Pages, 2022). A part of the light energy couples through the (gold) metal surface, where the electrons begin to move due to excitation. The electron movements are called ‘plasmons’. The oscillation of the electrons generates an electric field with a range of around 300 nm between the metal surface and the surrounding solution. Therefore, the refractive index changes taking place only near the metal surface are detected. The SPR angle is material-dependent, varying based on the refractive index of the material. It also depends strongly on the laser wavelength and optical properties of the prism and the sensor. If any small changes occur in the sensing medium, such as the attachment or binding of the molecules, the plasmons are not formed, and the detector can

measure the changes in the reflected light. (Nguyen et al., 2015). SPR measurements are recommended to be performed at least twice to guarantee their reliability (SPR-Pages, 2022).

The SPR angle is the angle of minimum reflectivity of the substance deposited on the sensor chip. The change in the SPR angle can be determined by altering the incident light angle. By increasing the incident light angle above the TIR angle, the formation of the plasmons begin, and the SPR phenomenon occurs. The reflected light intensity is recorded during the binding of ligands to a target. The ligands, for example, cells, antibodies, or peptides, deposited on the metal sensor surface must be immobilized before the sample solution is injected onto the sensor. The immobilized ligands may undergo a structural change by interacting with a target during the injection. The optical indicators detect the events on the biosensor, which are then recorded and monitored by the detector. Usually, the binding of the ligand to the target increases the refractive index at the surface of the metal sensor. The signal changes can be measured in response units (RU), one RU describing a critical angle shift of 10^{-4} degrees. Before injecting the sample, the initial RU value equals the starting critical angle. (Nguyen et al., 2015)

The association phase begins when the ligand binds to the target. The binding occurs when the collision between the ligand and target has the correct orientation and energy. The binding lasts for an unknown time. The dissociation phase begins when the ligand separates from the target. After the separation, both the molecules are identical to that they were before (SPR-Pages, 2022). The association- and dissociation phases are presented in Figure 5.

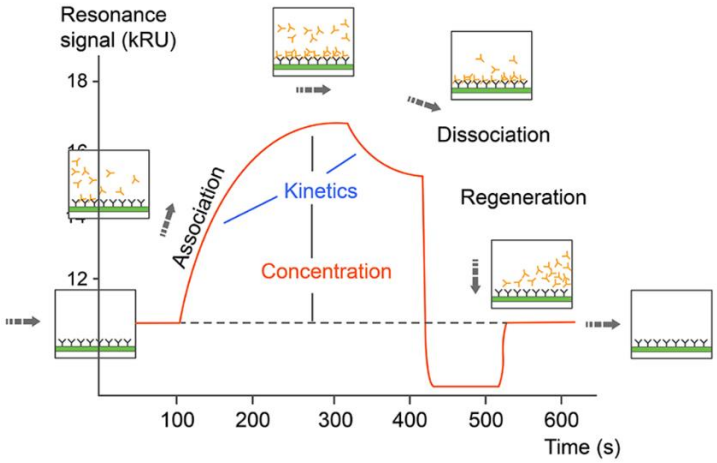

Figure 5. Phases of association and dissociation in a SPR sensorgram (CreativeBiomart, 2023). The association phase occurs during the beginning of the sample injection, when the interactions between the ligand and the target begin. The dissociation phase occurs when the ligands are separating from their targets.

The running buffer and its properties are particularly important features when planning the SPR experiments. The buffer contains the sample analyte which will bind to the target and, therefore, can markedly affect the interaction between them, for example, by its osmolality, composition, and pH-value. It is utmost important to have a flat buffer baseline before the experiment is started. The baseline drift can be detected by running the buffer in all the channels as long as needed (depends on the target). It should give a value of < ± 0.3 RU/min, and a low response, < 5 RU. The injection time of the sample solution is influenced by the association- and dissociation rates, as well as the concentration of the analyte solution. The analyte concentration in turn influences only the association phase. The time of the interaction should be so long that the association curve gives an adequate response, and the dissociation curve decays sufficiently. (SPR-Pages, 2022)

The surface plasmon resonance angle can be affected by the properties of the metal surface, the wavelength of the light, the refractive index of the media and temperature. Therefore, these properties should be defined, and the dependency be exploited when performing the measurements. If the light is not completely p-polarized, it will increase the background intensity and will not contribute to the excitation of plasmons. (SPR-Pages, 2022)

The surface plasmon resonance sensorgram gives a plot of SPR response vs. time. An example of the SPR sensorgram is presented in Figure 6B. The SPR sensorgram provides plenty of information regarding the measurement, for example, the binding event between an analyte and target, about the specificity of the binding, and information about the kinetics, affinity, and concentrations of the substances in question. Typical phases of the SPR sensorgram are baseline, association, steady-state, dissociation, and regeneration, as presented earlier in Figure 5. (Wong, 2020)

The minimum in the reflectance spectrum gives information of at which angle or wavelength the light is absorbed by the surface plasmons. An example of the SPR curve is presented in Figure 6A. The dip on the SPR curve shifts depending on the change in the refractive index, because of structural changes of the molecules (e.g., binding) on the sensor surface. The change in the reflected angle is dependent on the amount of the bound analytes from the solution, in other words mass increase. The increase in refractive index can be noticed by an

increase in the incident light angle required to excite surface plasmons. These changes in the SPR response are plotted as a function of time in a sensorgram. (Wong, 2020)

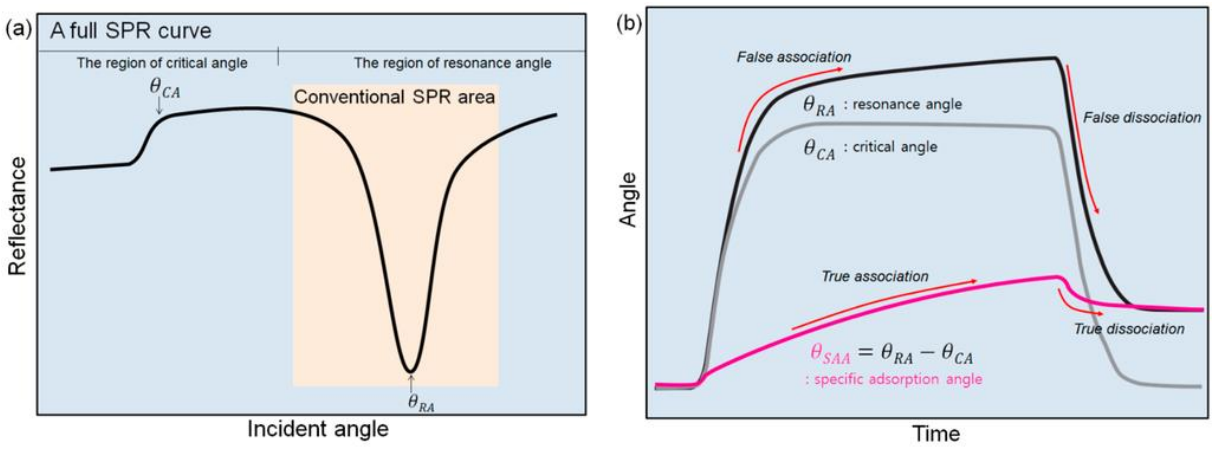

Figure 6A. An example of an SPR spectra and 6B. SPR sensorgram (Jang et al., 2015). SPR curve presents the full SPR spectra, showing the regions of critical angle (when all the incoming light reflects inside the prism) and resonance angle (dependent on the number of bound analytes) (SPR-Pages, 2022). SPR sensorgram presents different phases of the measurement as a function of time.

2.2. LigandTracer

LigandTracer is an instrument that can monitor molecular interactions in real time. The biggest difference between LigandTracer and SPR is that LigandTracer requires using of fluorescent substances for the measurements. The measurements can be performed with a few preparatory steps and, therefore, the instrument is usually quite simple to use. (LigandTracer, 2023)

General measurement steps contain labeling the ligand with a fluorescent substance, applying the Petri dish containing target molecules in a solution (often living cells), and after reaching the baseline (commonly after a few minutes), adding the sample solution to the dish. The interaction occurs usually within minutes to hours, depending on the nature of the measurement and the substances used. (LigandTracer, 2023)

The data from a LigandTracer instrument is generated by measuring the bound ligand concentration in a rotating dish. The dish contains the immobilized cells and the solution with a fluorescently labeled sample ligand, and the increase in the signal can be detected when the binding occurs. (Umeå University, 2023). A picture explaining the working principle of LigandTracer is presented in Figure 7.

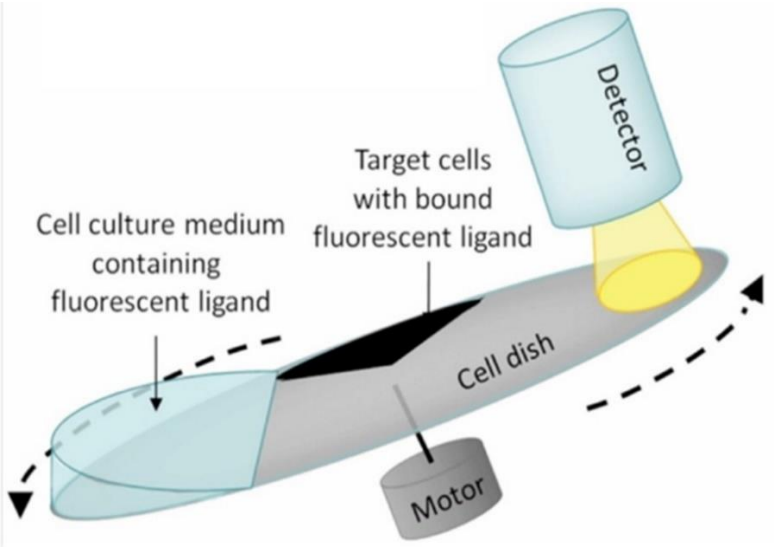

Figure 7. The principle of a LigandTracer instrument (Umeå University, 2023). The detector senses the signals on a rotating dish when the labeled analytes bind to their targets.

There are different kinds of LigandTracer instruments: green, yellow, grey, and white. The biggest difference between the instruments is the type of label they detect, but most of the applications can be performed with all the LigandTracer instruments. Different kind of applications include measurements such as affinity and kinetics of different interactions, specificity measurements, ligand-target interactions, conjugates and their properties or effects to each other, and how temperature affects the interaction. (LigandTracer, 2023).

Affinity and kinetics of interactions provide useful information, for example, in ranking drug leads or when investigating receptor systems. LigandTracer can be used for measuring the affinity of interactions, calculating the kinetic rate constants, measuring the ligand residence time, finding out the deviations from a one-to-one binding mode, or to investigate the saturated target concentration. The specificity measurements between a ligand and target

can be utilized, for example, when comparing or investigating the cell line or target specificity, or in epitope mapping applications. Ligand-target interaction measurements include, for example, target clustering and dimerization occasions. Analyzing the conjugates can be useful, for example, when studying antibody-drug conjugates, how they affect the affinity- and the binding kinetics, predictions of radiotracers, batch-to-batch variation, and ligand heterogeneity. Temperature often has a crucial role in (binding) kinetics, affinity, internalization rate and interactions, and it can be useful to investigate how it affects the measurement. Different biological signals can also be detected with LigandTracer, for example, the sequence of binding events, binding stability, signal initiation, and how the binding affects the magnitude of a biological signal. (LigandTracer, 2023). An example of data obtained from LigandTracer measurement is presented in Figure 8.

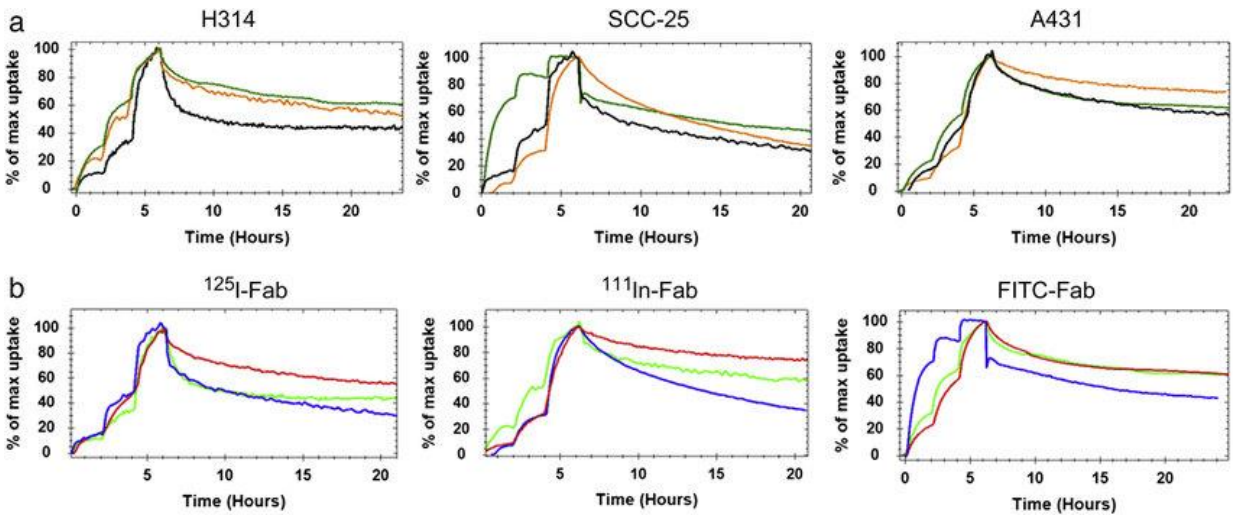

Figure 8. Different data got from LigandTracer measurements (Stenberg et al., 2013). The pictures show that different analytes produce different signals.

The instrument used in this project is LigandTracer Green, which is widely used in detection and quantification of biomolecular interactions, such as to monitor the interactions between antibodies and cells, protein-protein-, protein-tissue-, and bacteria-cell interactions (Umeå University, 2023).

2.3. Confocal microscopy

Confocal microscopy has become an extremely popular imaging method during the recent years. It has multiple advantages, such as the instrument is relatively easy to use considering its high-quality images and several applications it can be utilized for. It has been claimed that confocal technology is “one of the most important advances ever achieved in optical microscopy”. (Olympus Lifescience, n.d.). A typical instrument setup is presented in Figure 9.

Figure 9. Basic confocal instrument setup (Warwick University, 2017).

Confocal microscopy can be used to image both fixed and living cells and tissues (Olympus Lifescience, n.d.). Therefore, it has widely utilized in biomedical sciences, but also in material sciences. There are also several types of confocal microscopes, distinguished by their scanning method: laser scanning confocal microscopes, spinning disc confocal microscopes, and hybrid scanning confocal microscopes (Elliott, 2020). In this project, the focus is on the laser scanning microscope.

The principle of basic light microscopy techniques is to image the samples that are altered to an illuminating light, which passes uniformly through the sample over the field of view (widefield microscopy). It has a relative strong risk to generate blurred images due to the out-of-focus light, especially when imaging thicker samples. If any fluorescence substances are used in the imaging process, all the dye molecules are stimulated, also the ones in out-of-focus planes. The significant difference between the basic technique and the confocal microscopy technique is that confocal microscopes can reject the out-of-focus light from the detector, leading to a possibility to image high-resolution images also of thicker tissues. A confocal microscope focuses on the same diffraction-limited spot of the sample and generates the complete image by moving the spot over the sample and collecting data with one layer at a time to build a complete image. (Elliott, 2020). The difference between confocal- and widefield fluorescence microscopy images is presented in Figure 10.

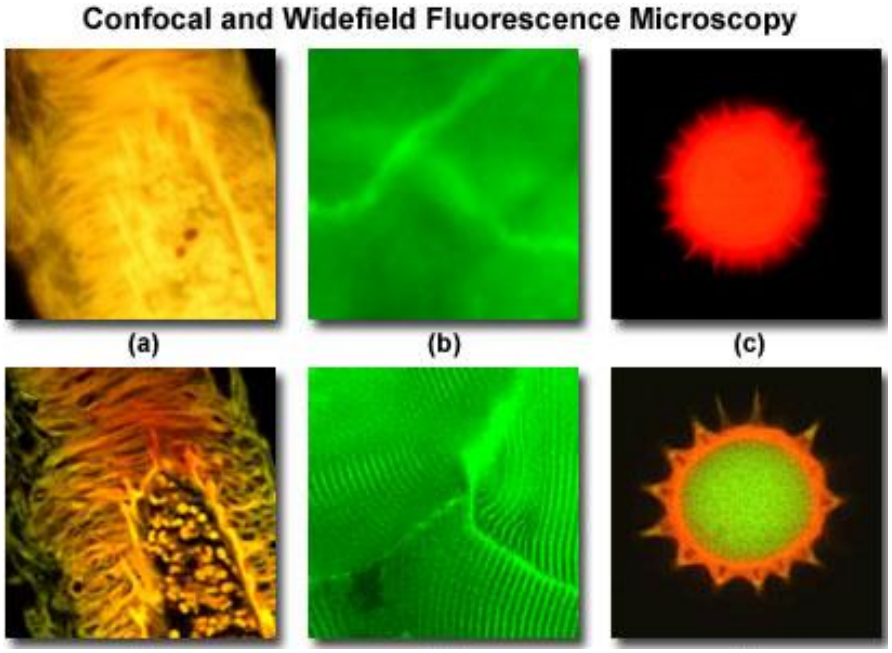

Figure 10. The difference between widefield fluorescence microscopy (upper row) and confocal microscopy (bottom row) (Olympus Lifescience, n.d.). The images taken with a confocal microscope are much more exact and accurate.

Components typically needed for a confocal microscope setup are the pinholes, the objective lenses, low-noise detectors, fast scanning mirrors, filters for wavelength selection, and laser illumination. There are several different types of lasers: argon, helium-neon, diode, fiber, and

solid-state lasers. The gas lasers are still widely utilized, even if the solid-state lasers are more stable, produce less heat, have a better uniformity, and emit broader range of visible wavelengths. The illustrated differences between widefield fluorescence- and confocal microscopes are presented in Figure 11.

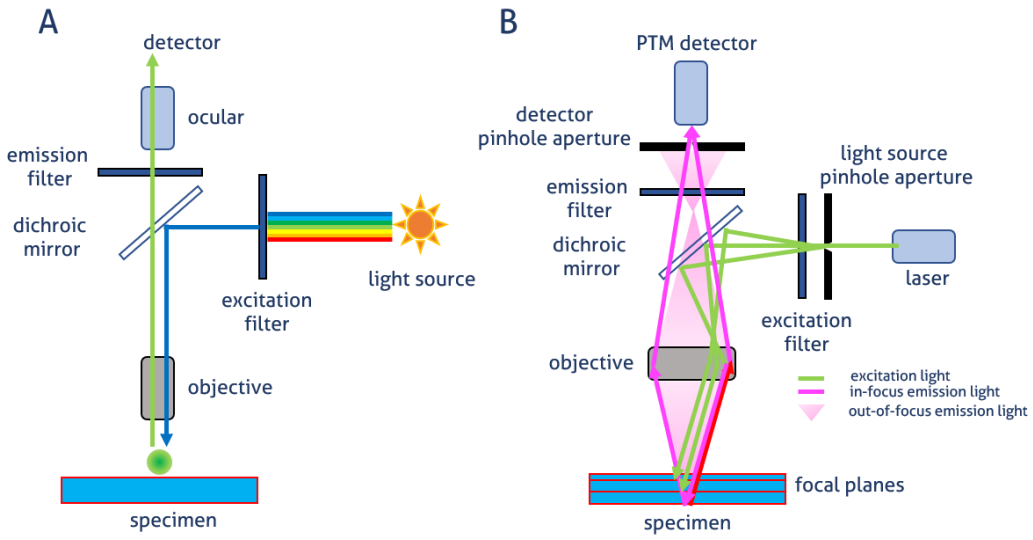

Figure 11. The difference between widefield fluorescence- (A) and confocal (B) microscope instruments (Proteintech, 2022). The biggest difference between the instruments is that confocal technology prefers a laser source, and widefield fluorescence a basic light source.

The numerical aperture, NA, is a factor by which the resolution is typically determined in light microscopy. The best resolution that can be achieved with a confocal microscope is ~ 0.2 µm laterally and ~ 0.6 µm axially. (Elliott, 2020). The equations that can be utilized in determining lateral and axial resolution are:

$$R_{lateral} = \frac{0.4\,\lambda}{NA}$$

$$R_{axial} = 1.4\,\lambda\,\eta/(NA)^2$$

R= resolution, λ= emission light wavelength, η= refractive index of the mounting medium, NA= numerical aperture of the objective (Elliott, 2020).

The advantages of the confocal microscope technique are as follows:

- the image quality of a confocal microscope is excellent
- the signal-to-noise ratio is improved
- the light-scattering technique enables the reducing of image blurring
- electronical adjustment of magnification possible
- enables a clear examination and 3D reconstruction
- effective Z-axis scanning

The disadvantages are that the process might be more time-consuming, and the image acquisition procedure is often more complicated. (Proteintech, 2022)

2.4. Biological protein drugs

2.4.1. Immunoglobulin G

Immunoglobulin G (IgG) is the most frequent immunoglobulin class in humans. The molecule consists of two heavy chains, two light chains and the Fc-region (Nezlin, 1998). The primary function of IgG in humans is to bind to the antigens from the Fab region (Painter, 1998). IgG can also bind to the Fc receptors on the target cells, e.g., macrophages (Nezlin, 1998). By binding to the cell surface receptors of multiple different cell types, IgG can contribute the phagocytosis process, effectuate the overall antibody synthesis and result in the antibody-dependent cellular cytotoxicity (ADCC) (Painter, 1998). IgG1 subclass is widely utilized in developing therapeutical antibodies (Thomson, 2016). The structure of the IgG molecule is presented in Figure 12.

IgG is used as a negative control in this project. These molecules can be used as a control to reveal any possible non-specific background signals of the studied monoclonal antibodies. Primary antibody background signals can be caused, for example, by binding to the Fc receptors on the target cells. (ThermoFisher c), 2023). IgG do not have a relevant specificity to the target antigen in this project (EGFR).

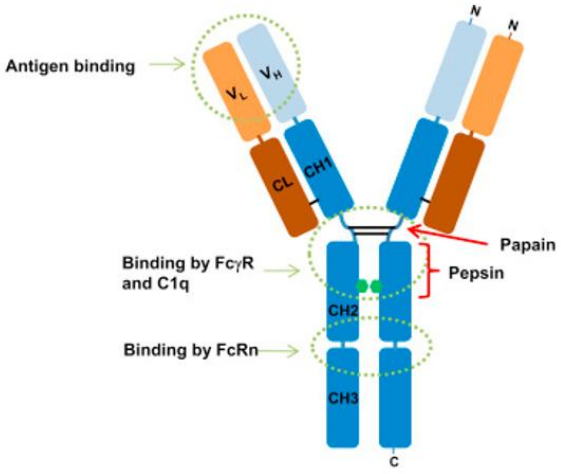

Figure 12. The structure of IgG (Thomson, 2016).

2.4.2. Trastuzumab

Trastuzumab is a humanized monoclonal antibody, that binds to the human epidermal growth factor -receptor ($EGFR_2$), also known as HER_2 -receptor (Drugbank a), 2023). The monoclonal antibodies are proteins that have high specificity and affinity for the molecule they are generated against. A humanized antibody (such as trastuzumab) is generated by implanting murine protein loops within human immunoglobulins (Malik and Ghatol, 2023). Trastuzumab is classed as a recombinant IgG1 kappa antibody, which means that it has a heavy chain of the immunoglobulin class G, and a modified region in the kappa (κ) light chain (Biolabs, 2017; Drugbank a), 2023). The structure of trastuzumab is presented in Figure 13.

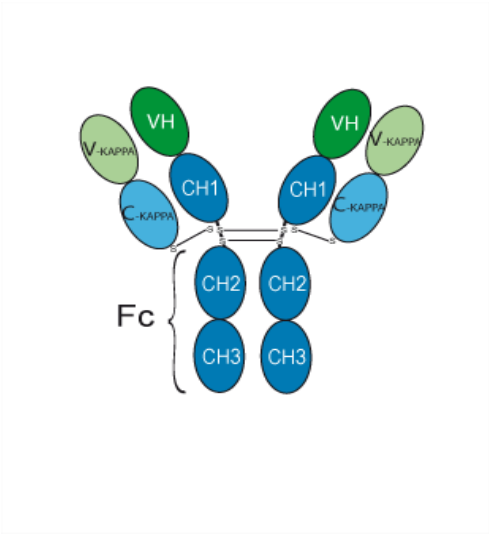

$C_{6470}H_{10012}N_{1726}O_{2013}S_{42}$

Figure 13. The chemical formula and the protein structure of trastuzumab (Drugbank a), 2023).

Trastuzumab binds selectively with high affinity to the extracellular domain of the HER_2 -protein (Trastuzumab, Drugbank, 2023). It also has anti-human antibody properties, including binding to the primary antibodies. That can, for example, aid the detection, sorting, and purification of the target antigens, by improving the signal that leads to higher sensitivity and selectivity. (AAT Bioquest, 2021; Drugbank a), 2023)

Trastuzumab is widely used as a treatment of the human epidermal growth factor receptor (HER_2) positive metastatic breast cancer, e.g., with an over-expression of the HER_2 protein in tumors. As much as about 20–30% of breast cancers are estimated to arise from the abnormal activity or the over-expression of the HER_2. The activation of the HER_2 in cancer cells triggers several different downstream pathways, which may lead to an abnormal proliferation of the cells. Cancer cell growth and proliferation can be directly and indirectly affected by and suppressed with trastuzumab. (Trastuzumab, Drugbank, 2023). Trastuzumab can also facilitate the antibody-dependent cellular cytotoxicity (ADCC), where the effector cells recognize the antibody-coated cells expressing the tumor-derived antigens on their surface, leading to the death of the cancer cell (Gómez Román et al., 2014; Greenblatt and Khaddour, 2023).

Trastuzumab is also used to treat metastatic breast cancers in combination with other treatment methods and to treat metastatic gastric cancer (EMA, 2018). EGFR-2 is over-expressed in appr. 10-25% of gastric cancer cases (Gunturu et al., 2013).

2.4.3. Cetuximab

Cetuximab is a recombinant chimeric monoclonal antibody (mAb), that binds competitively to the epidermal growth factor receptor (EGFR). It is classed as a human/ mouse immunoglobulin G1 mAb, and its structure is presented in Figure 14. (Drugbank b), 2023).

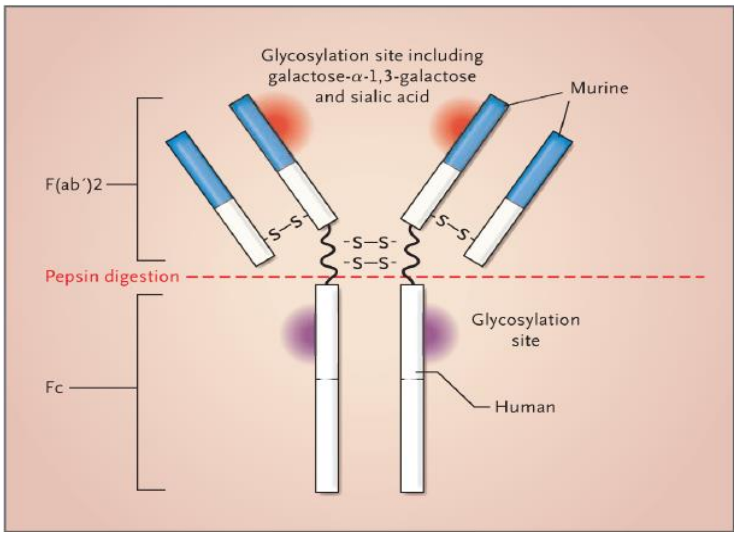

$C_{6484}H_{10042}N_{1732}O_{2023}S_{36}$

Figure 14. The chemical formula and the protein structure of cetuximab (Drugbank b), 2023; ResearchGate, 2008).

Binding of cetuximab to the epidermal growth factor receptor competitively inhibits the binding of the epidermal growth factor (EGF) to the receptor (Drugbank b), 2023). Normally, the binding of the EGF to the EGFR controls the cell-growth and induces the cell-signaling pathways leading to cell division. In cancer cells, the mutated and over-expressed EGFR can cause the cancer cells to divide uncontrollably. (NCI, 2011). The inhibition of the EGFR signaling

pathways leads to the down regulation of the cell cycle progression and cell survival. The binding of cetuximab to the EGFR also induces cell apoptosis (cell death) and inhibits the production of the cell growth factors, as well as promotes the antibody-dependent cellular cytotoxicity, similarly as trastuzumab. (Drugbank b), 2023)

Cetuximab is used to treat the metastatic EGFR involved colon- and rectum cancer, that contain non-mutated versions of a RAS -gene family. It can be used as a single therapy or together with other treatments depending on the cancer type. It can also be used to treat squamous-cell cancers in the head and neck, such as the mouth, throat, or larynx, usually as a combination therapy with, for example, radio therapy.

3. AIMS

The aims of this master's thesis project are presented as follows:

1. To grow the cell cultures containing SK-OV-3 ovarian cancer cells, overexpressing both EGFR- and HER_2 receptors, and study how biological, protein-based drugs trastuzumab (HER_2 inhibitor), cetuximab (EGFR inhibitor), and the negative control (IgG protein) interact with these cells.

2. To assess if the multi-parametric surface plasmon resonance (MP-SPR) technique is suitable for measuring and recording these interactions in real time, and if the measured MP-SPR signals could be used to differentiate between the surface interaction and the internalization of the biologicals in SK-OV-3 cells.

3. To use complementary confocal microscopy and LigandTracer techniques to validate the results of the MP-SPR measurements.

4. MATERIALS AND METHODS

4.1. Materials

4.1.1. Materials for the cell cultivation process

The SK-OV-3 (human adenocarcinoma) cell line used in this thesis was obtained from ATCC, the Global bioresource center (SKOV3 ATCC, 2022). The cell line was stored in -80 °C before cultivation. McCoy's 5A Medium (LOT: 70043059, 500ml), obtained from ATCC was used as the cell culture medium (ATCC, 2022). The cell culture medium was stored at 4 °C. The medium contained 1.5 mM L-glutamine and 2200 mg/l sodium bicarbonate, and the following substances were added: 8 ml 1M Hepes (in 0.85% NaCl, Gibco, Thermofisher scientific, UK), 50 ml heat inactivated Fetal Bovine Serum (FBS) (Gibco, Thermofisher scientific, Brazil), 5 ml L-glutamine 100X (200mM, EuroClone, Europe), 5 ml penicillin/streptomycin antibiotics (10,000 U/ml, Lonza, Germany).

Hepes (25mM) was used to achieve the extra buffering capacity for cells that were manipulated outside the CO_2 incubator for longer periods. L-glutamine provides nutrition, stimulates the growth, and prolongs the viability of the cells. Antibiotics are used to prevent bacterial contamination of both gram-negative and gram-positive bacteria. FBS is used to provide essential growth factors to the cells. (ThermoFisher b), 2023).

Initially, the Thermo Scientific Nunc Easyflasks (75cm^2) were used in the cell cultivation process. The Cellstar cell culture dishes 145x20 mm and 100x20 mm were used later in the process. Other substances needed for the subculturing procedure of the cells were: Phosphate buffered saline (PBS), obtained from Lonza, USA, and stored at 4 °C. Trypsin-EDTA (1X, 0.25%), was obtained from Gibco and stored at -20 °C.

4.1.2. Drug substances for the measurements

Herceptin, with a concentration of 20.3 mg/ml trastuzumab was obtained from Roche. The drug solution was stored at -80 °C before the aliquoting process. The aliquots were diluted in 1xPBS solution and stored at -20 °C.

Erbitux (Merck KGaA), with a concentration of 0.82mg/ml cetuximab was obtained from InvivoGen. The drug solution was stored at -80 °C before the aliquoting process. The aliquots were diluted in 1xPBS solution and stored at -20 °C. Another batch of cetuximab was obtained from MedChemExpress (LOT: #244070). The drug solution was stored at -20 °C before the aliquoting process. The aliquots were diluted in 1xPBS and stored at -20 °C.

Human IgG Isotype Control, with a concentration of 11.6 mg/ml in PBS was obtained from Invitrogen (product code: 31154). The drug powder was stored at -80 °C before the aliquoting process. The aliquots were diluted in 1xPBS solution and stored at -20 °C.

4.1.3. Materials for the MP-SPR measurements

The gold sensors used for the MP-SPR measurements were obtained from BioNavis (metal layer: Au, substrate type: OPL, number of sensors: 8, lot: BN-AVR-2011-005). The instrument used for the MP-SPR measurements was a custom built BioNavis MP-SPR instrument with four flow channels and two laser wavelengths (i.e., 670 nm and 785 nm) for each flow channel, equipped with a four-channel peristaltic pump (Ismatec MS-4/12 Reglo Digital Pump), presented in Figure 15. The unique feature of the MP-SPR instrument compared to traditional SPR instruments is that the MP-SPR records the full SPR curve over a wide angular range. This enables measurements with thick layers such as cells, which is not possible with any other SPR instrument on the market. The software programs used for data collection and management were the MP-SPR-Navi Control (version 6.7.0.0.) and the MP-SPR Navi Data Viewer (version 6.7.0.1.) programs, respectively.

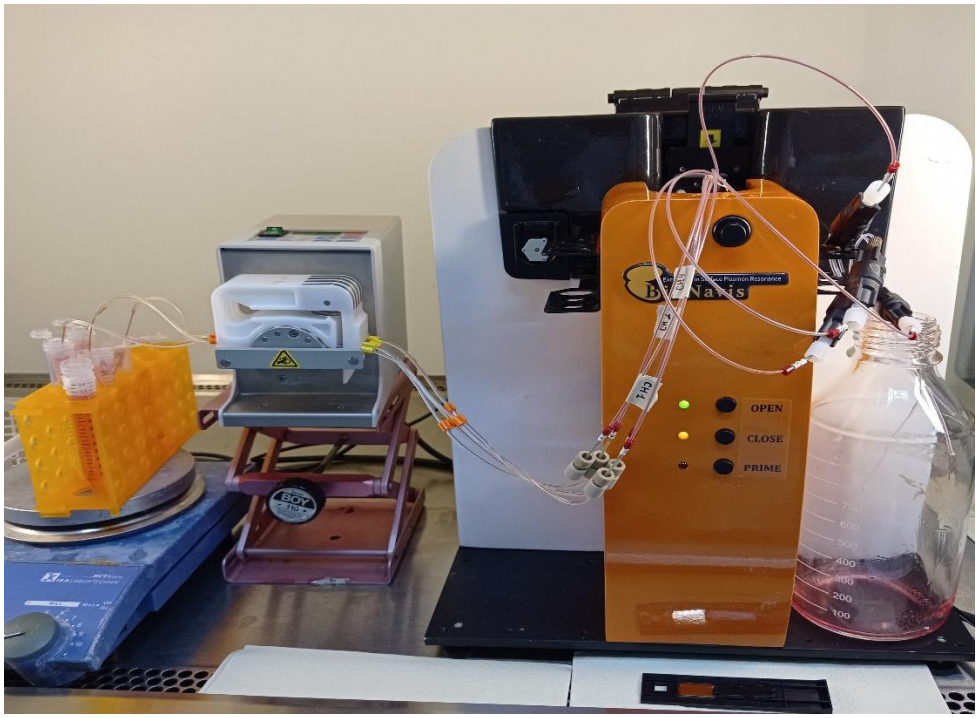

Figure 15. The instrument that was used for the MP-SPR measurements (Osmonen, 03/2023).

Gold sensors were cleaned before cell seeding in a boiling solution containing 3 ml hydrogen peroxide (30% wt in H_2O, 216763-500ml, Sigma-Aldrich), 3 ml ammonium hydroxide (28-30% NH_3basis, 221228-500ml-A, Sigma-Aldrich) and 15 ml Milli-Q water. The cells were cultivated in the cleaned gold sensors in Corning Incorporated Costar 6-well plates. Before the measurements, the cell coated sensors were moved to BioLite 35mm Tissue culture dish plates (Thermo Scientific) containing cell medium with 25 mM of added Hepes. The Finnsonic Ultrasonic Cleaner M12 instrument was used to degas the medium solutions before MP-SPR measurements. Hellmanex III (2%) solution from Hellma analytics and 70% Ethanol was used to clean the instrument between measurements.

The fibronectin used as an adhesion promoter for cells on the gold sensors during cell seeding on the sensors was originally from human origin, but due to delivery problems of the supplier, bovine plasma fibronectin was used instead (lyophilized, 1ml, obtained from Gibco, stored at -20 °C). The running buffer for the MP-SPR measurements (SPR medium) was prepared by adding 1M Hepes 0.85% in NaCl (Gibco, Thermofisher scientific, UK) to McCoy's 5A Medium (LOT: 70043059, ATCC) to achieve a concentration of 25mM.

4.1.4. Materials for LigandTracer measurements

The LigandTracer Green (Ridgreview instruments ab, Sweden) equipped with a green fluorescence detector (526 nm) was used for interaction kinetics measurements of labeled antibodies. The labelling of the antibodies with a fluorescence substance was performed with a Thermo scientific Pierce FITC antibody labeling kit (53027). The kit contained the following components for labelling the antibodies: FITC fluorescein isothiocyanate (3x 50 µl), borate buffer (0.67M, 1 ml), and purification resin (5 ml). The LigandTracer Control software (version 2.4.0.) was used for the measurements and the data were handled and analyzed with the TraceDrawer software (version 1.9.2.). FITC-protein-ratios after labeling were measured with a NanoDrop 2000 instrument.

4.1.5. Materials for the confocal microscopy measurements

SK-OV-3 cells were cultivated on a cellview glass bottom cell culture dish 35/10 mm (Greiner bio-one). Microscopy measurements were performed with a Zeiss LSM 880 confocal microscope by using a 63x oil objective and Diode 405 nm- and HeNe 633 nm lasers.

The samples for the confocal measurements were prepared by using PBS to wash the cell-coated plates before applying any other solution, paraformaldehyde 4% for fixing the cells, 0.1% triton-100 as a permeabilization solution, primary antibodies (i.e., the samples) diluted in the MP-SPR buffer solution, a fluorescent secondary antibody: Thermo Fisher scientific Alexa Fluor 633 goat anti-mouse IgG (H+L), and DAPI (4',6-diamidino-2-phenylindole, 10 µg/ml) for staining the nucleus.

4.2. Methods

4.2.1. The cell cultivation process

The SK-OV-3 cells were thawed from the -80 °C storage by strictly following the thawing procedure, described in *Appendix 1* (Thawing Frozen Cells, n.d.).

First, the cell culture medium was replaced every two days to ensure that the cells started to grow as expected. The condition of the cells was monitored daily with a microscope until the 100x20mm cell plate was almost completely covered with cells. The subculturing protocol based on the information on the manufacturer's website, described in *Appendix 2* (SK-OV-3 ATCC, n.d.), was strictly followed every time the cell culture was split. Figure 16 presents the cell density of SK-OV-3 cells in the beginning of the culture and after three days of culture.

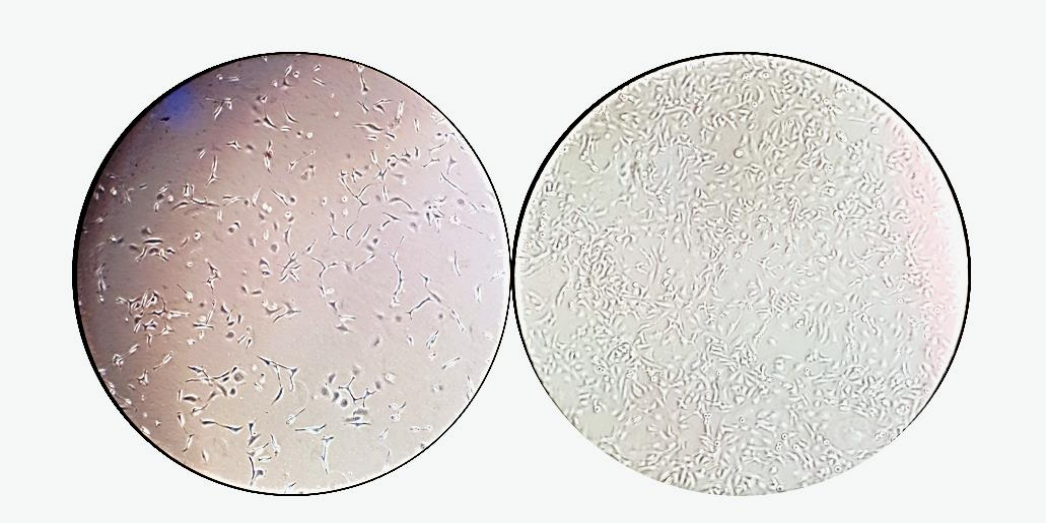

Figure 16. Cell density of the SK-OV-3 cells in the beginning of the project and after three days of culture (Osmonen, 01/2023).

After the cells began to grow and divide normally, the seeding on gold sensors for MP-SPR measurements were started. The cells were cultured continually during the entire thesis process, and the cell cultures were split twice a week. A back-up cell culture was always available in case of any destruction of the used cell cultures. A stock of generation 5 cells was

prepared and stored at -80 °C for future purposes. Cell generations up to passage 22 were used for the MP-SPR measurements. The LigandTracer- and confocal microscopy measurements were performed with a new batch of generation 5 cells that were thawed from the -80 °C storage according to the thawing procedure described in *Appendix 1.*

4.2.2. Sample aliquoting process

The trastuzumab batch obtained from Orion Pharma had a concentration of 20mg/ml in a volume of 60 µl in 1xPBS (total amount 1.2 mg). The molecular weight of trastuzumab is 145,531 g/mol (Drugbank a), 2023). Consequently, the concentration of the stock solution was 137.4 µM. To make the concentration of the stock solution more rational, the solution was diluted to 100 µM by adding 1xPBS.

After diluting the trastuzumab solution to 100 µM, the total volume of the stock solution was 82.44 µl. From this, five stocks of 10 µl each were aliquoted and stored at -20 ℃. These were used for preparing the base solutions of 1 µM for the MP-SPR measurements by adding 990 µl of the MP-SPR running buffer. The desired concentration for every measurement was reached by diluting the 1 µM base solution with the MP-SPR running buffer.

The cetuximab batch obtained by Orion Pharma had a concentration of 0.82 mg/ml in a volume of 100 µl in 1xPBS (total amount 0.82 mg). The molecular weight of cetuximab is 145,781.6 g/mol (Drugbank b), 2023). Consequently, the concentration of the stock solution was 5.62 µM. To make the concentration of the stock solution more rational, the solution was diluted to *5* µM by adding 1xPBS. After diluting the cetuximab solution to 5 µM, the total volume of the stock solution was 112.4 µl. From this, four stocks of 20 µl each were aliquoted and stored at -20 °C. These were used for preparing the base solutions of 1 µM for the MP-SPR measurements by adding 80 µl of the MP-SPR running buffer. The desired concentration for every measurement was reached by diluting the 1 µM base solution with the MP-SPR running buffer. Another batch of cetuximab used for the measurements had a concentration of 5 mg/ml, and it was diluted to a stock solution with a concentration of 1 µM by using 1xPBS and stored at -20 °C.

The IgG batch of 100 µg was obtained from Orion Pharma in a powder form. The powder was dissolved in 1xPBS with a volume of 0.1 ml according to the instructions of the manufacturer. Consequently, the concentration of the stock solution was 6.67 µM. To make the concentration of the stock solution more rational, the solution was diluted to 6 µM by adding 1xPBS. After diluting the IgG solution to 6 µM, the total volume of the stock solution was 111.7 µl. From this, four stocks of 20 µl each were aliquoted and stored at -20 °C. These were used for preparing the base solutions of 1 µM for the MP-SPR measurements by adding 100 µl of the MP-SPR running buffer. The desired concentration for every measurement was reached by diluting the 1 µM base solution with the MP-SPR running buffer.

4.2.3. Preparation of the cell-coated sensors

The gold sensors used for the MP-SPR measurements were always cleaned for 5 min in a boiling cleaning solution containing hydrogen peroxide, ammonium hydroxide and Milli-Q water. Sensors were placed with the gold side downwards during the cleaning and maximum two sensors were cleaned at the same time. The cleaned sensors were then rinsed with Milli-Q water and stored for maximum one week in a 3 ml Eppendorf tube filled with 70% ethanol.

After the cleaning procedure, the sensors were kept in 70% ethanol for at least 12 hours before moving them inside the laminar hood to avoid any contamination. Before passaging the cells, the sensors were leaned against the wall of a 6-well plate to let the ethanol evaporate. At this point, the fibronectin solution with an appropriate concentration was prepared. Normally three sensors were seeded at the same time, which was considered when calculating the concentration of the fibronectin solution. Each well in the 6-well plate containing a cleaned sensor for cell seeding was filled with 2 ml of fibronectin solution. Thus, a total volume of 6 ml of the fibronectin solution was needed. The stock solution of fibronectin had a concentration of 1 mg/ml. The coating concentration of fibronectin needed for each well was 2.5 µg/cm^2 and the area of each well was 9.5 cm^2. Therefore, the volume of the fibronectin needed for three sensors was: 2.5 µg/cm^2 x 9.5 cm^2 x 3 wells = 71,25 µl. This volume of the stock fibronectin solution was pipetted into a falcon tube containing 6 ml-71,25 µl= 5928.75 ml of 1xPBS.

After the evaporation of the ethanol, the sensors were placed into the wells and washed twice with 1xPBS (2ml for each well). The fibronectin solution was then pipetted into the wells with the sensors and allowed to interact with the sensors at least 30 minutes, while the regular passaging of the cells was proceeded according to the Subculturing procedure protocol *(Appendix 2)*. One million cells were seeded into each well and the 6-well plate containing the sensors was then incubated in the cell incubator overnight at 37 °C (5% CO_2). The growth medium was always changed the day after the seeding procedure and a microscope was used to guarantee that the cells had attached to the sensor. The sensors were used for MP-SPR measurements three days after the seeding.

4.2.4. MP-SPR measurements

The MP-SPR measurements were performed using a custom built BioNavis multi-parametric surface plasmon resonance instrument. The tubing and the flow channels of the instrument should always be cleaned after each measurement, and to guarantee the cleanliness of the tubes and flow channels, water was always injected for 15 minutes with a speed of 100 µl/min with a plain gold sensor prior to starting the measurements with the cell coated sensor. The temperature was set to 20 °C, 35 °C or 37 °C, depending on the requirements of the measurement. While the pre-cleaning process with water was running and the temperature of the instrument was adjusting to the set temperature, the sensor with the cells was moved in a separate BioLite 35 mm Tissue culture petri dish containing 2 ml of the SPR medium to allow the cells to adapt to the different medium. The sensor was then brought out from the cell laboratory to wait for the measurement.

After water had been injected for ca. 15 minutes during the pre-cleaning process, the running buffer in the MP-SPR instrument was changed to the SPR medium, which was injected for ca. 10 minutes with a speed of 100 µl/min. The SPR medium was always degassed with the Finnsonic Ultrasonic Cleaner M12 instrument to minimize the formation of air bubbles. When the SPR medium started to continuously flow from all the flow channel outlets, the pump was stopped, flow cell was opened, and the plain gold sensor was replaced with the cell coated

sensor. The backside of the sensor was first wiped with 70% ethanol and then dried with a dry paper. Eventually, the cell coated sensor was carefully inserted into the instrument.

After the cell coated sensor was inserted, the flow cell was closed, and the flow speed of the running buffer was set to 30 µl/min. The 'full range' scan was always selected first to guarantee that the full SPR curve had the proper shape. The measurement was then started with 'custom' settings. The SPR angle scan range was set between 58 to 77 degrees. Before the injection of the samples, the cells were allowed to stabilize, which usually took between 120-180 minutes. After a stable baseline of the MP-SPR signal was achieved, then the samples containing trastuzumab, cetuximab, and/or IgG were injected for ca. 30 minutes, 4 hours or overnight depending on the measurement. After every measurement, the instrument was cleaned with Hellmanex III 2% solution, 70% ethanol, Milli-Q water, and air. Each of these cleaning solutions was injected for at least 5 minutes with a speed of 100 µl/min.

4.2.5. Ligand tracer measurements

LigandTracer measurements were performed with a LigandTracer Green instrument, equipped with a green fluorescence detector (526 nm). FITC labelled proteins were prepared using the instructions of the Pierce FITC antibody labeling kit. The procedure consisted of three steps: protein preparation, protein labelling and protein purification.

Briefly, 40 µl of the Borate buffer (0.67M) was added to 0.5 ml of the protein samples (2mg/ml, diluted in PBS). The protein samples were labelled with the FITC reagent by adding 0.5 ml of the prepared protein samples to the vial of the FITC reagent. The protein samples and FITC dye were then mixed properly by pipetting and vortexing.

After mixing, the vials containing the protein samples and FITC reagent were centrifuged briefly (1 minute) to collect the sample to the bottom of the vial. The mixtures were then incubated for 1 hour at room temperature, protected from light. After the incubation, the 6 spin columns were placed in separate microcentrifuge collection tubes and the Purification resin (400 µl) was added to the mixtures. The mixtures were centrifuged for ca. 1 minute at 1000 x g to remove the storage solutions.

The columns were then placed in new collection tubes and 265 µl of the labeling reaction was added to each column. The solutions were mixed properly by pipetting and vortexing before centrifuging (30 seconds at 1000 x g) to collect the labeled proteins. All the solutions which contained the same protein were combined with each other, and the used columns were discarded. The labeled proteins were stored protected from light at 4 °C for one week (max. one month).

The concentrations (FITC-to protein estimations) were measured with a NanoDrop 2000 instrument. Protein concentrations of 4nM and 12nM, diluted in the SPR medium were used for all the samples (trastuzumab, cetuximab and igG). After reaching a baseline signal (ca. 25-30 minutes), the association measurements were started with 4nM samples, which were injected for 2-3 hours, i.e., as long as the signal remained at a high level. After that, the 12nM samples were injected equally. To measure the dissociation phase, plain SPR buffer solution was injected for 2-3 hours at the end of the measurement.

4.2.6. Confocal microscopy measurements

Confocal microscopy measurements were performed with the assistance of a doctoral student. To test a suitable concentration of the samples to be used in the measurements, test pictures of AlexaFluor labeled trastuzumab 3nM and 12nM were first taken and compared with each other. The confocal images obtained during this pre-screening showed that the images were clearer with the higher concentrations. Consequently, the concentration of 12nM was chosen to be used for all proteins in all the confocal microscopy measurements. The samples and time points used in the confocal microscopy measurements were: trastuzumab 12nM (1 hour and 24 hours), cetuximab 12nM (1 hour, 4 hours, 24 hours), and IgG 12nM (1 hour and 4 hours). Three to five images of each sample were taken and saved on a memory stick.

Confocal measurements were performed by two different methods. In the first method, the SK-OV-3 cells were cultured on a cellview glass bottom cell culture dish until the cell layer had 60-80 % confluence (usually 2-3 days). The dish was then washed twice with 1xPBS (1000 µl) before incubating the cells with 500 µl of 12nM of the primary antibody (trastuzumab,

cetuximab and IgG in SPR buffer) in each dish. The samples were allowed to incubate with the cells for 1, 4, or 24 hours at 37 ℃. After the incubation the dish was washed two times with 1xPBS (1000 µl) and fixed with 4% paraformaldehyde (400 µl) at room temperature for 20 minutes. The dish was then washed three times with 1xPBS (1000 µl). All the tips and liquids containing rests of paraformaldehyde were collected to separate vials.

Permeabilization was performed using 0.1% Trixon-X-200 at room temperature for 10 minutes. The dish was then washed three times with 1xPBS (1000 µl). Secondary antibody incubation was then performed by adding 500 µl of a fluorescent secondary antibody (Alexa Fluor 633 goat anti-mouse IgG, 1:1000 in PBS) in the dark and allowing it to incubate for 1 hour. The dish was then washed three times with 1xPBS (1000 µl), and once with Milli-Q water (1000 µl). Nuclear staining was performed by adding DAPI (500 µl) and allowing it to incubate at room temperature for 10 minutes. The dish was then washed three times with 1xPBS (1000 µl). The sample was stored at 4 ℃ in 1xPBS (1000 µl) and covered with aluminum foil.

In the other method used for confocal microscopy measurements, the labelled protein sample solutions prepared with the ThermoFisher FITC kit for LigandTracer measurements were utilized. Hence, the permeabilization and secondary antibody incubation steps were not performed in these measurements. Confocal microscopy measurements were performed with both types of protein samples (labeled with AlexaFluor and FITC reagents) to see if any differences in cell interactions could be detected with differently prepared labeling protocols and protein samples.

4.2.7. Data management

Data in this project was obtained from the surface plasmon resonance-, confocal microscopy-, and Ligand tracer measurements and from online articles and literature. The data is presented in the form of ASCII data, pictures, diagrams, and text. This research did not use or assess any sensitive data such as private or other restricted data, nor imposed any ethical or copyright issues. Data was obtained continuously during the project, and the information and recordings of the measurements were added daily to the laboratory diary word file, which is protected with a password.

Data from the MP-SPR measurements was saved on the computer connected to the MP-SPR instrument and saved as a text file to a memory stick, from which the file could be converted to desired excel diagrams. Data from the LigandTracer measurements was saved on the computer connected to the LigandTracer instrument, modified with TraceDrawer, and saved to a memory stick, from which the file could be converted to desired excel diagrams. Data from the confocal microscope was saved on the computer connected to the microscope and saved in a picture format to a memory stick, from which the data could be copied into BioImage XD program and converted to a usable form.

Data was then monitored and added to the master's thesis word file whenever more results were obtained. The file was saved as a word file on a password- protected computer, and the copy of the file is saved online on the OneDrive, which is also protected with a password. The results and the final file of the master's thesis will be shared with Orion Pharma, and published online by Åbo Akademi University, which also owns the rights of this project.

5. RESULTS

5.1. The MR-SPR measurements

All in all, 19 SPR measurements were performed with variable results and success. A usual (and desirable) appearance of the full SPR curve is presented in Figure 17. The round shape of the curve at around 65 degrees and the large angular position of the main SPR peak at around 72 degrees shows that the cells are present on the sensor. The form of the full SPR curve presenting the reflectance intensity as a function of angle is similar for all the channels, which indicates that the cell monolayer in each channel is similar and that everything is in order to perform the MP-SPR measurements.

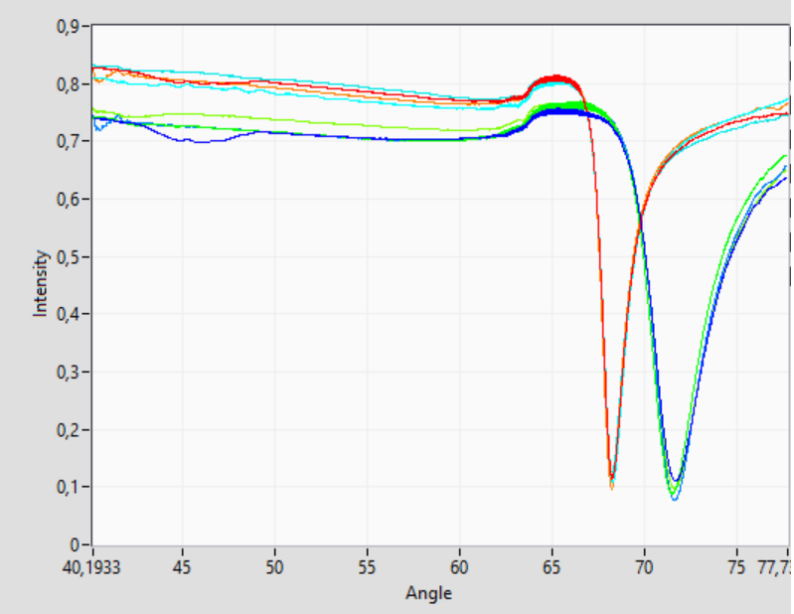

Figure 17. A usual appearance of the full SPR curve (Osmonen, 2023).

Figure 18 presents microscopy pictures of the SK-OV-3 cells immobilized on the gold sensor before and after the MP-SPR measurement. It is clearly seen that some of the cells have died, i.e., have a rounder morphology and the cells in the flow channel where the solution has been injected have become flatter after the MP-SPR measurement.

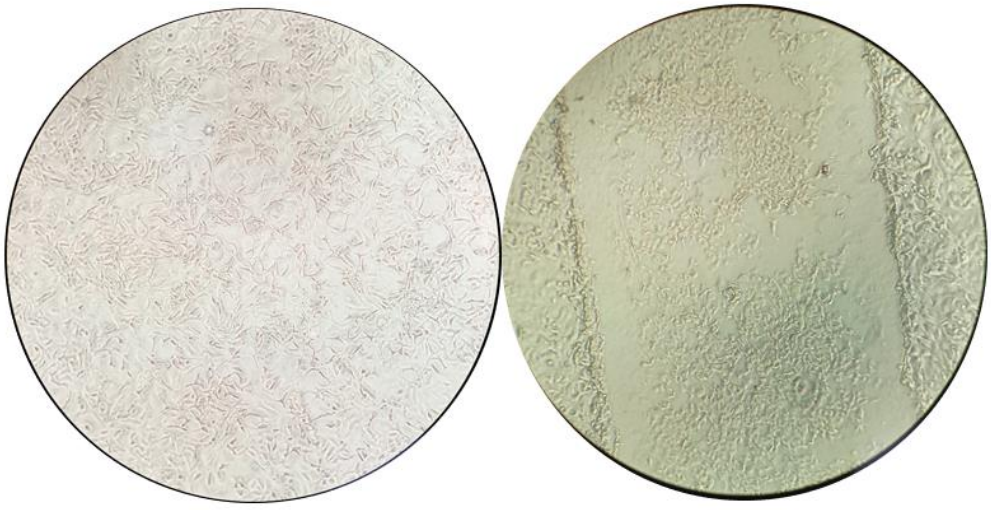

Figure 18. SK-OV-3 cells on the gold sensor before the MP-SPR measurement (left image) and after the measurement (right image) (Osmonen, 02/2023).

Figures 19, 20 and 21 present the MP-SPR signal responses measured at 20 °C during 20-minute injections of trastuzumab, cetuximab and IgG. The sensorgrams of trastuzumab show that there is a clear decrease and levelling out of the signal responses during the 20-minute injections. The decrease in the signal response is due to the contraction of cells during trastuzumab interaction which could indicate that trastuzumab mainly interacts with the cell surface and is not taken up by the cells. There is hardly any difference in the magnitude of the signal response when comparing the lower concentration (3nM) with the higher concentration (6nM). This could be due to that the cell surface interactions of trastuzumab have already reached a saturation point at these concentrations.

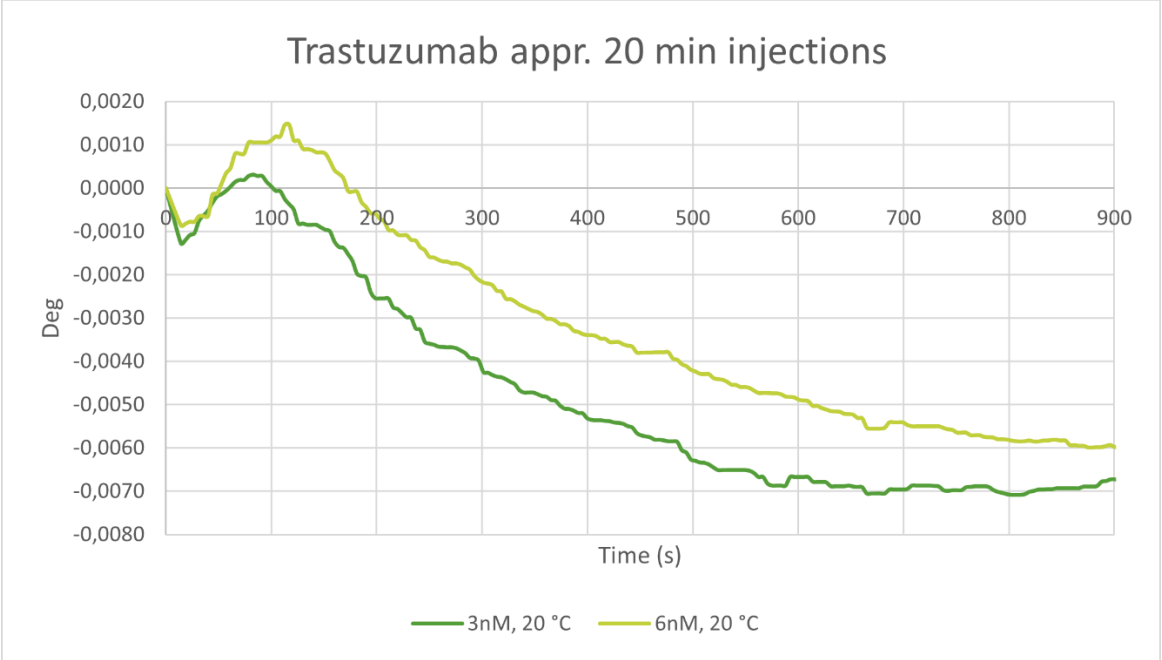

Figure 19. MP-SPR signal responses of two concentrations of trastuzumab (3nM and 6nM) during interaction with SK-OV-3 cells (Osmonen, 2023).

The sensorgrams of different concentrations of cetuximab (Figure 20) measured at 20 °C show that there is a clear increase followed by a slow decrease and levelling out of the signal responses during the 20-minute injections. The cetuximab sensorgrams have a clear concentration dependent behavior where the signal response increase with increasing concentration. Also, the signal response at the end of the measurements stays at a higher level the higher the concentration is when comparing to the baseline level. This indicates that there is an initial interaction of cetuximab with the cell surface that causes the cells to spread on the sensor (initial increase in signal), which is followed by cell uptake of cetuximab (slight decrease in signal ending up on a higher level than the baseline.

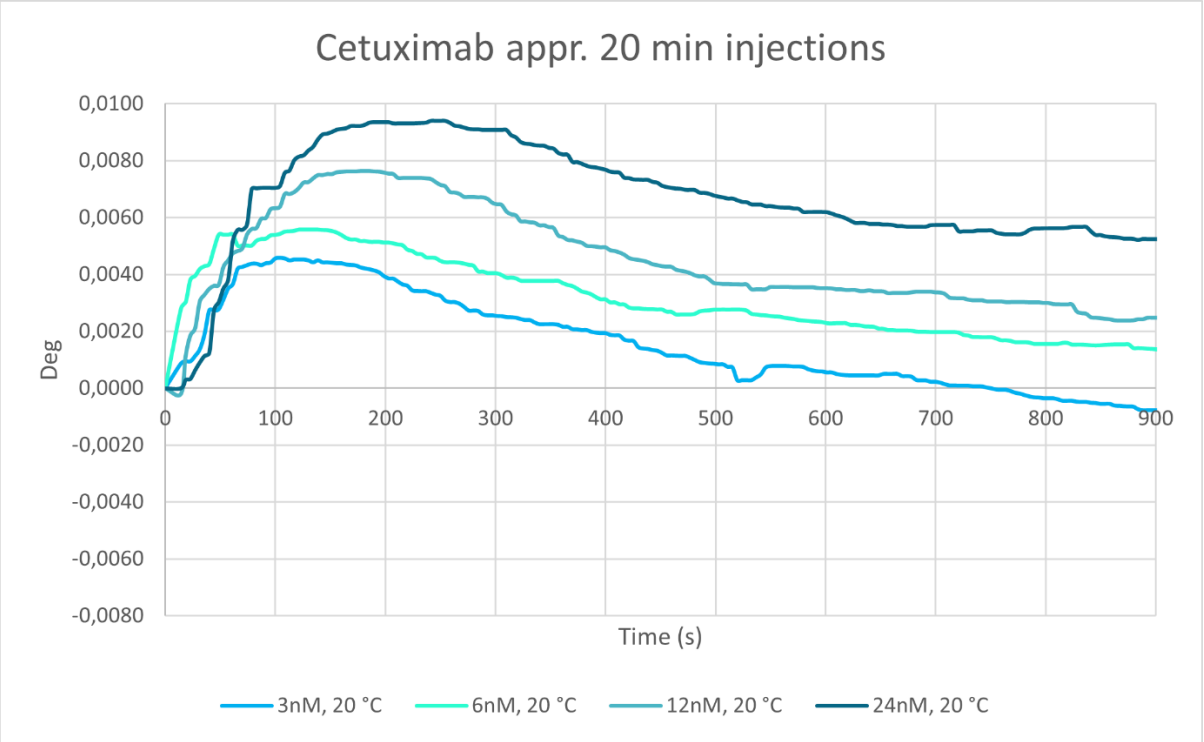

Figure 20. MP-SPR signal responses of four concentrations of cetuximab (3nM, 6nM, 12nM and 24nM) during interaction with SK-OV-3 cells (Osmonen, 2023).

The sensorgrams measured for IgG at 20 °C (Figure 21) gives particularly variable results, as the same concentration (6nM) gives both a negative and a positive signal response. This could indicate that the interaction of IgG with the cells is not so strong and that the drift between day-to-day measurements is too large to distinguish the interaction for IgG at low

concentrations. However, the higher concentration (24nM) leads to clearly higher signal response than the lower concentration (6nM). The high signal response for 24nM IgG resembles the signal response for cetuximab at 24nM (Figure 20), although the signal response at the end of the measurement is slightly lower for IgG compared to cetuximab. This indicates that IgG has a similar mode of action on the cells, i.e., causing spreading of cells and that it is possibly also taken up by the cells.

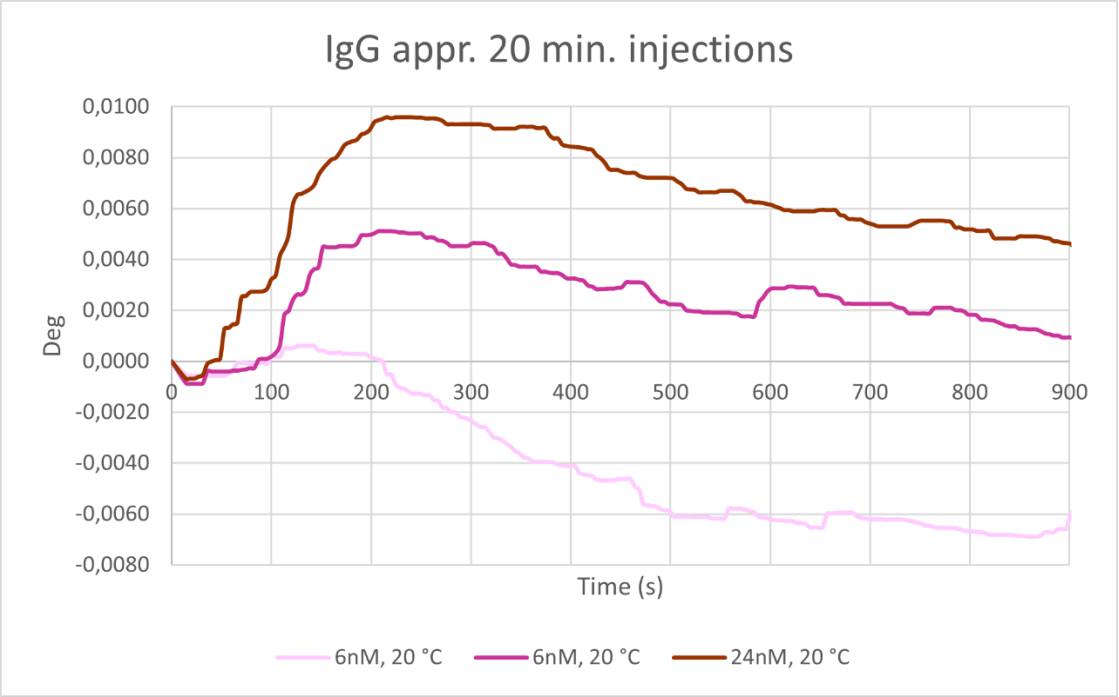

Figure 21. MP-SPR signal responses of two concentrations of IgG (6nM and 24nM) during interaction with SK-OV-3 cells (Osmonen, 2023).

Figure 22 presents the MP-SPR signal responses during 4-hour injections of all the protein samples with a concentration of 12nM at 20 °C and 35 °C. The signal responses are extremely variable, as there is almost nothing in common between the sensorgrams of the same protein at different temperatures, even if the concentrations were kept the same.

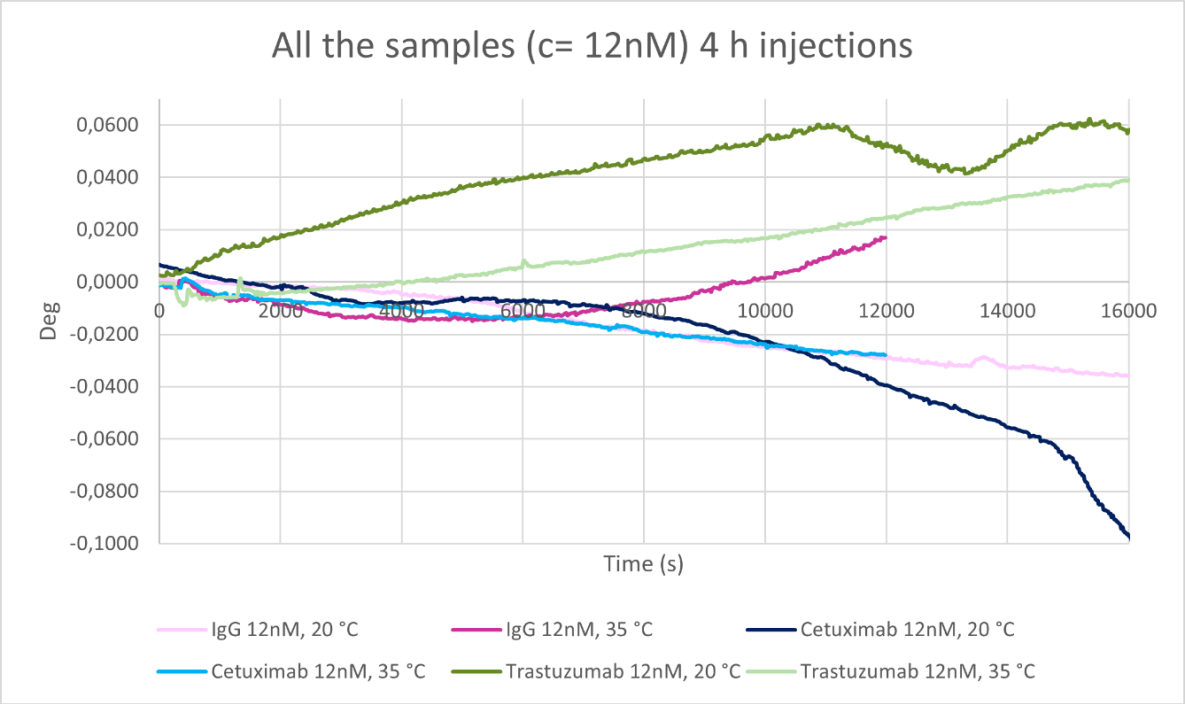

Figure 22. MP-SPR signal responses measured at 20 °C and 35 °C of all protein samples (12nM) during interaction with SK-OV-3 cells (Osmonen, 2023).

5.2. LigandTracer

Complementary measurements to MP-SPR measurements were performed with the LigandTracer Green technique once for all the three proteins. The LigandTracer signal responses for trastuzumab (4 and 12nM) during interaction with SK-OV-3 cells are presented in Figure 23. Trastuzumab gave a clear response for both concentrations and there was first a fast but rather small decrease in the signal followed by a slower decrease in the signal during the dissociation phase starting at ca. 350 min. The affinity of trastuzumab towards the SK-OV-3 cells was fitted with a one-site-binding model and was 1.6 x 10^{-10} M (Figure 23).

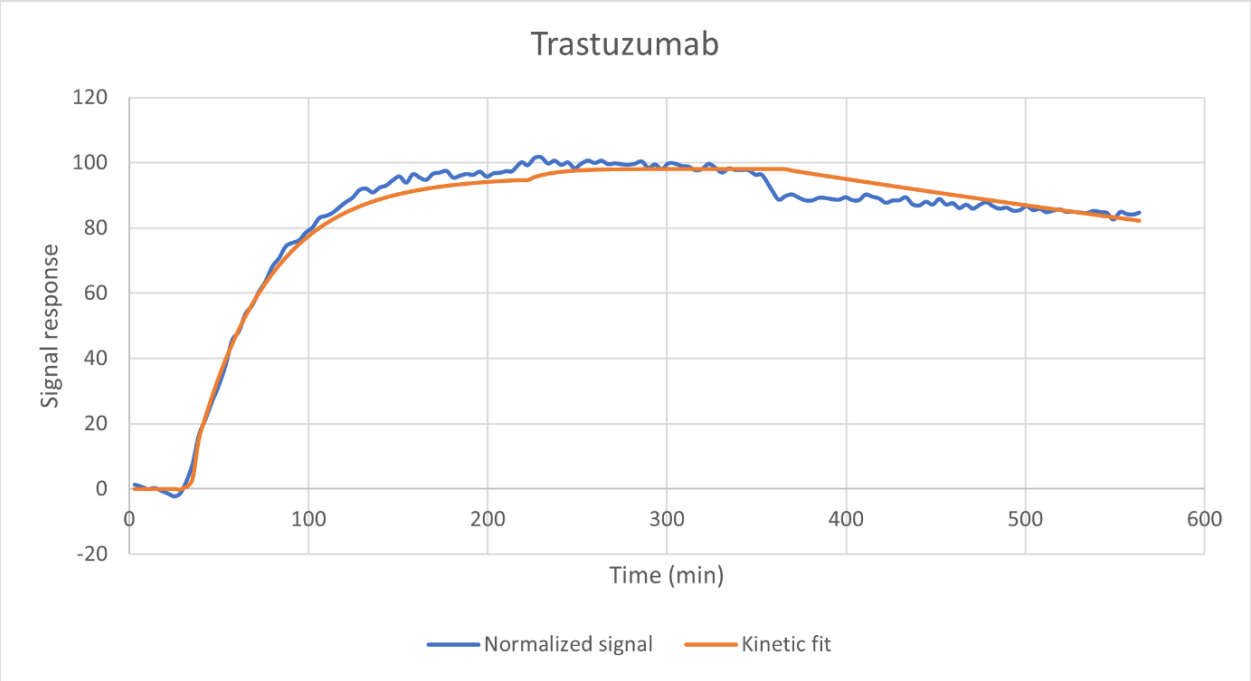

Figure 23. LigandTracer signal response during trastuzumab interaction with SK-OV-3 cells, original signal (blue) and normalized fitted data (red). The association phase includes trastuzumab samples of 4nM at t = 30 min, 12nM at t = 210 min and the dissociation phase was started at t = 350 min (Osmonen, 2023)

The LigandTracer signal responses for cetuximab (4 and 12nM) during interaction with SK-OV-3 cells are presented in Figure 24. Cetuximab also gave a clear response for both concentrations and there was practically no reduction in the signal response during the dissociation phase staring at ca. 240 min. The affinity of cetuximab towards the SK-OV-3 cells was fitted with a one-site-binding model and was 1,4 x 10^{-9} M (Figure 24).

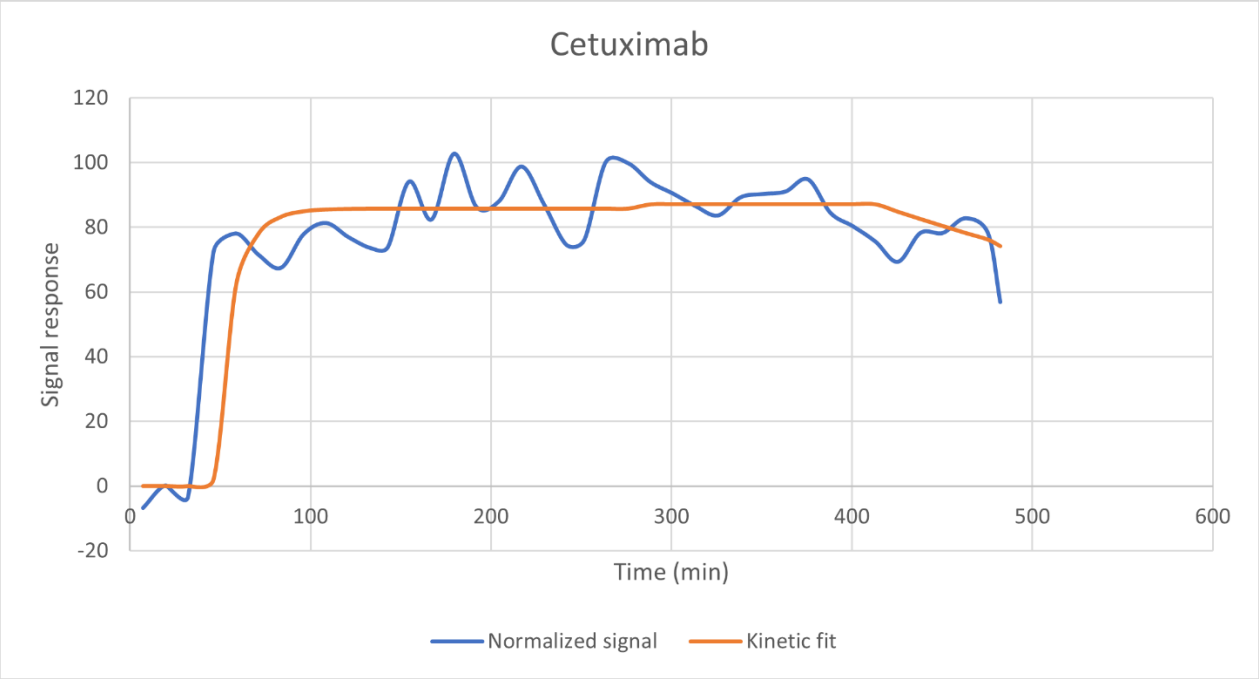

Figure 24. LigandTracer signal response during cetuximab interaction with SK-OV-cells, original data (blue) and normalized fitted data (red). The association phase includes trastuzumab samples of 4nM at t = 30 min, 12nM at t = 150 min and the association phase was started at t = 240 min (Osmonen, 2023).

IgG did not give any clear response in the LigandTracer measurements, as seen in Figure 25, which presents the LigandTracer signal responses of all the proteins. The results indicate that IgG do not interact with the SK-OV-3 cells in any larger extent. Thus, no further analysis was performed on this data.

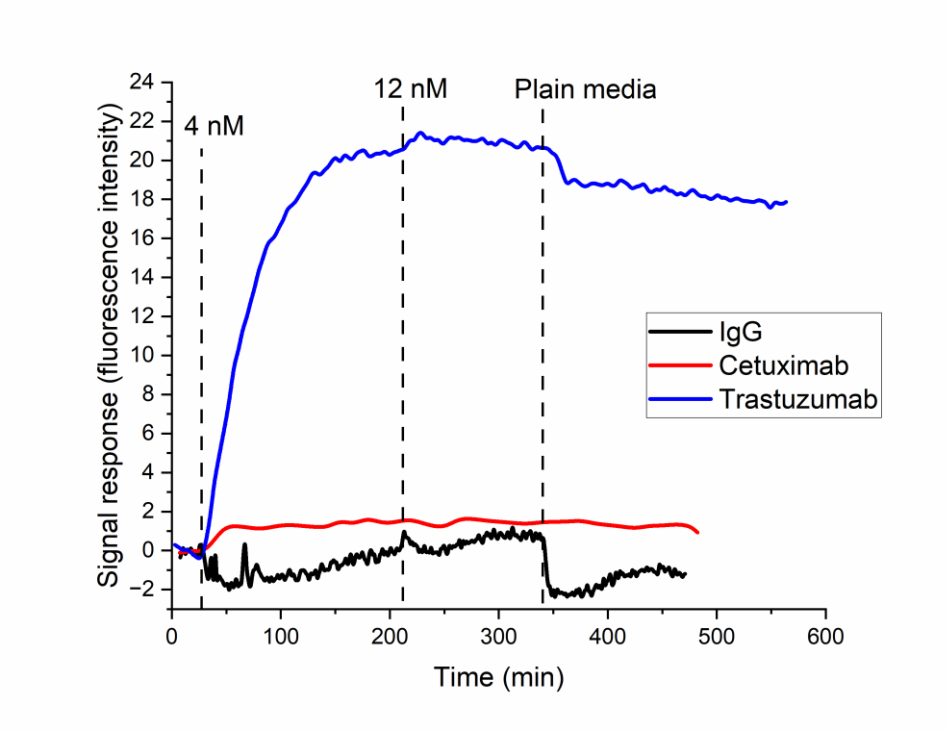

Figure 25. LigandTracer signal responses of all the proteins. IgG (12nM) has clearly lower interactions with SK-OV-3-cells than trastuzumab and cetuximab (Osmonen, 2023).

5.3. Confocal microscopy

Confocal microscopy was performed with both directly FITC labeled proteins and by using a secondary antibody (Alexa Fluor 633) to detect non-labelled proteins. The results obtained from the confocal microscopy measurements are presented in Figures 26, 27 and 28. The horizontal rows (A, B and C) are each presenting three images of the same sample, taken from the same spot. The first image is presenting the cell nucleus, which is colored with DAPI (blue). The second image in the horizontal row presents the protein sample, which is labeled with either FITC or AlexaFluor. The third image in the horizontal row presents the merged image of the SK-OV-3 cells with each protein.

All the proteins are colored with different colors by utilizing BioImageXD program. Trastuzumab is colored with green, cetuximab with pink and IgG with yellow. The SK-OV-3 cells nuclei have been stained with DAPI (blue color).

Figure 26 presents trastuzumab (green) labeled with FITC and AlexaFluor and the SK-OV-3 cells whose nuclei have been stained with DAPI (blue). Trastuzumab clearly accumulates on the cell membrane and shows a significant surface interaction with the cells. Some of the protein also end up in the cell nucleus. As seen in Figure 27, cetuximab has weaker interactions with the cell membrane, but is more readily accumulated inside the cells compared to trastuzumab, and IgG (in Figure 28) has no noticeable interactions with the cell membrane, nor is taken up by the cells.

The interactions between the SK-OV-3 cells and the different protein samples show the same trend despite the use of different fluorescent substances (Alexa Fluor or FITC). However, the images of the FITC-labeled trastuzumab are slightly clearer and more precise than the AlexaFluor-labeled images. Cetuximab seems to spread more extensively in the FITC-labeled images. IgG is having a slightly more noticeable interaction with the SK-OV-3 cells when the secondary antibody (Alexa fluor-labeled) was used compared with FITC-labeled samples.

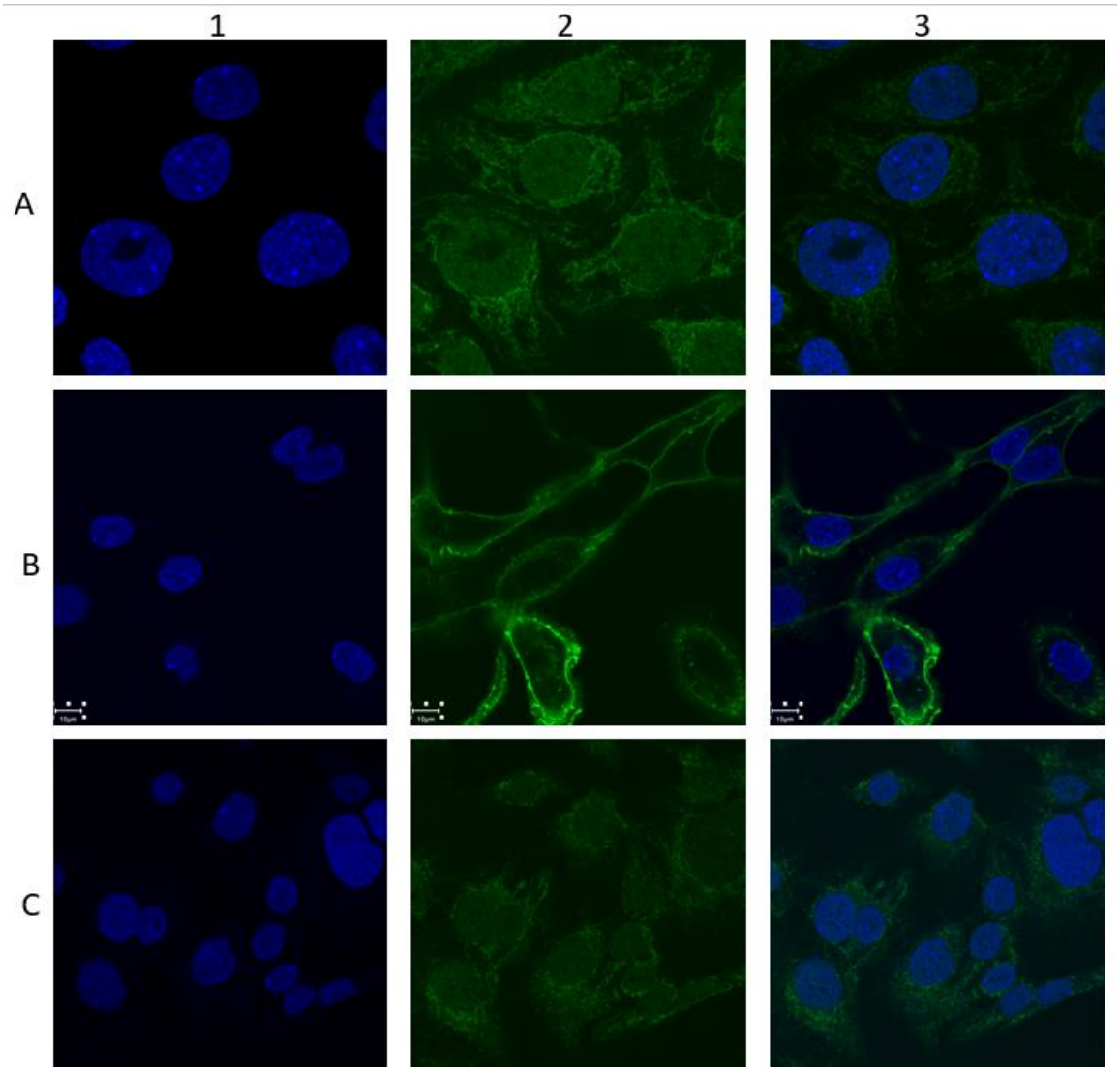

Figure 26. Confocal microscopy images of trastuzumab and SK-OV-3 cells (Osmonen, 2023). The horizontal row A presents trastuzumab, 1-hour sample, labeled with AlexaFluor. The row B presents trastuzumab, 4-hour sample, labeled with FITC. The row C presents trastuzumab, 24-hour sample, labeled with AlexaFluor. The cell nuclei of each sample are presented in the longitudinal row 1. The protein (trastuzumab) is presented in the longitudinal row 2. The cells and the protein are merged in the longitudinal row 3. The scale bar in the image is 10 μm.

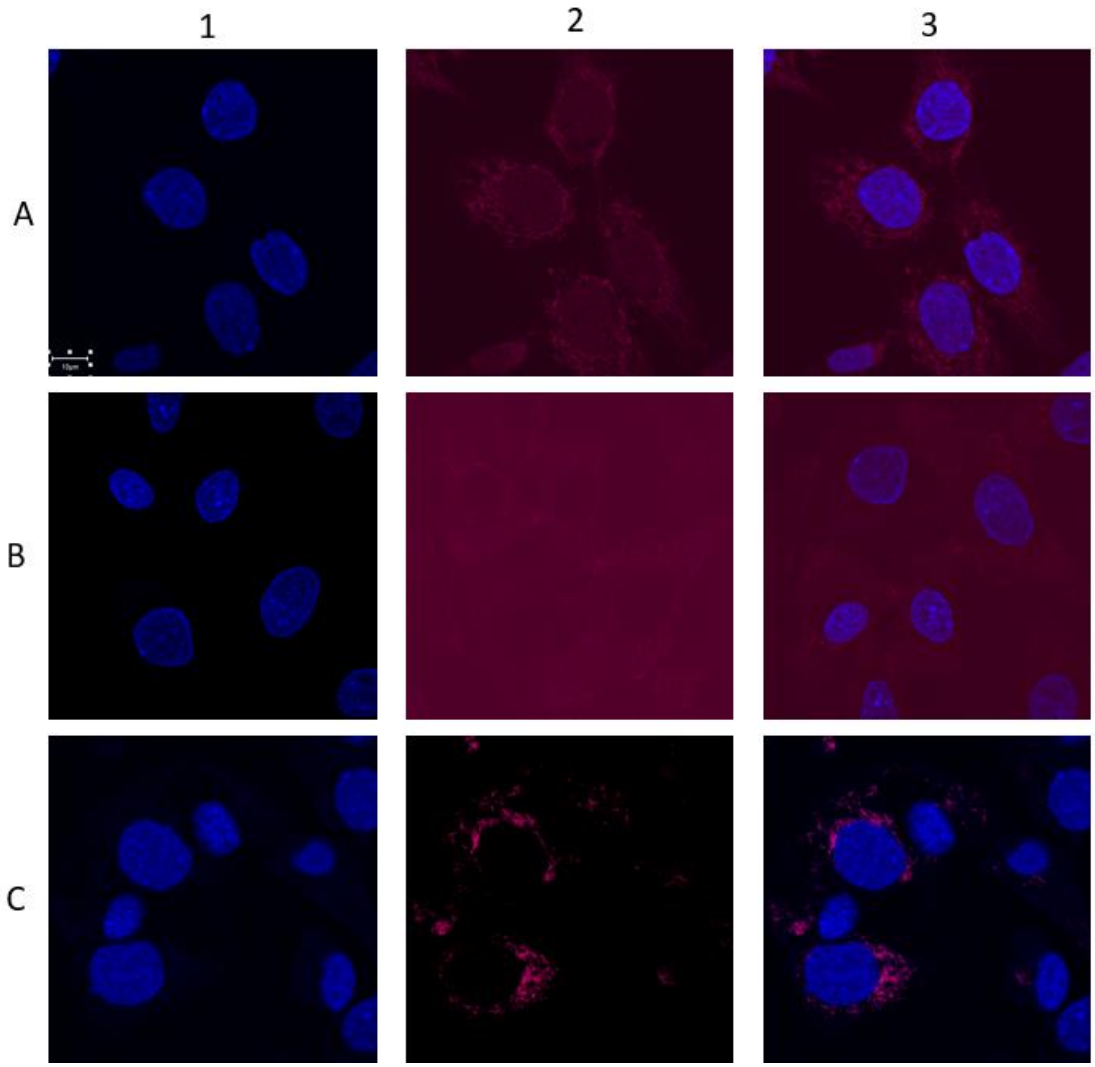

Figure 27. Confocal microscopy images of cetuximab and SK-OV-3 cells (Osmonen, 2023). The horizontal row A presents cetuximab, 1-hour sample, labeled with AlexaFluor. The row B presents cetuximab, 4-hour sample, labeled with FITC. The row C presents cetuximab, 24-hour sample, labeled with AlexaFluor. The cell nuclei of each sample are presented in the longitudinal row 1. The protein (cetuximab) is presented in the longitudinal row 2. The cells and the protein are merged in the longitudinal row 3. The scale bar in the image is 10 μm.

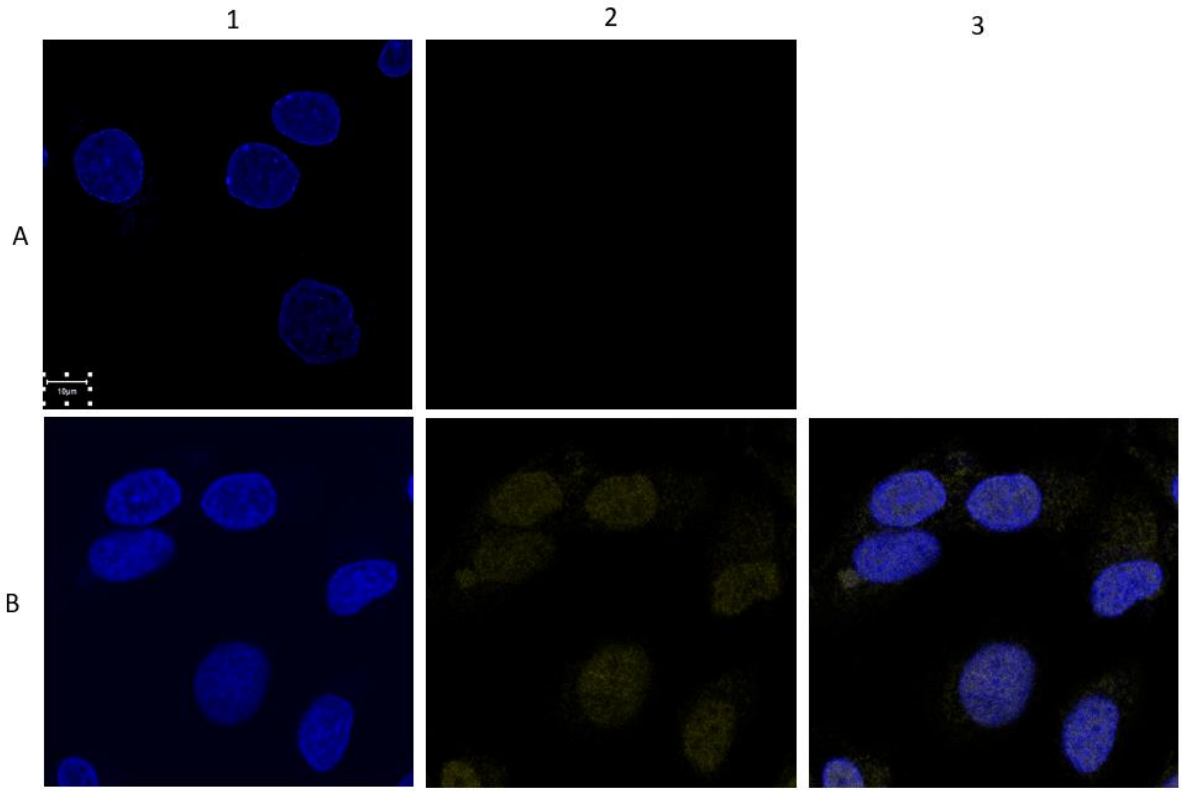

Figure 28. Confocal microscopy images of IgG and SK-OV-3 cells (Osmonen, 2023). The horizontal row A presents IgG, 4-hour sample, labeled with FITC. The row B presents IgG, 4-hour sample, labeled with AlexaFluor. The cell nuclei of each sample are presented in the longitudinal row 1. The protein (IgG) is presented in the longitudinal row 2. The cells and the protein are merged in the longitudinal row 3. The scale bar in the images is 10 μm.

6. DISCUSSION

The results from the MP-SPR measurements were extremely variable. The first measurements were performed in 20 °C, because many air bubbles was formed in the MP-SPR flow channels when measurements were attempted in 37 °C. The injections in 20 °C were kept short (20 minutes) to clarify if any differences between the samples could be seen in the first place. There are small differences that can be noticed between the protein samples, and for the same protein sample with different concentrations. However, the differences are not as great as was anticipated before beginning the project.

The problems with the air bubble formation were tried to be solved by heating the sample solutions that were injected into the MP-SPR flow channel in a water bath (appr. 37 °C), and by heating the instrument to 35 °C. The formation of air bubbles continued even though the tubes were continuously replaced for the peristaltic pump controlling the liquid flow in the MP-SPR instrument. The longer measurements are not considered to be reliable because of the problems induced by air bubbles and because of other problems of the instrument or cell culturing conditions that could not be recognized. The longer measurements were not replicable at all.

The MP-SPR results from the 20-minute injections are presented in figures 19-21. The most notable difference between trastuzumab and cetuximab is that trastuzumab gives negative and cetuximab positive MP-SPR signal responses. This can be due to that trastuzumab has a stronger tendency to interact with cell surface receptors that are not so readily internalized (HER_2), and that the interaction of trastuzumab with HER_2-receptors on SK-OV-3 cells induces contraction of the cells. Whereas, in the case of cetuximab, which interacts primarily with the readily internalizing EGF-receptor, the interaction induces spreading of the cells as well as accumulation of cetuximab inside the cell. The internalization rates of EGF- and HER_2 receptors have been studied by e.g., (Hendriks et al., 2003). A negative MP-SPR signal response have previously been addressed to contraction of cells during drug stimulation, while a positive MP-SPR signal response have been addressed to cell spreading, accumulation of material in cells and/or redistribution of intracellular mass closer to the sensor surface (Suutari et al., 2016; Viitala et.al., 2013). As a matter of fact, this type of behavior can also be seen from the confocal microscopy images (Figures 26, 27 and 28) where the cell nuclei in the case of cetuximab is larger compared to the cell nuclei for trastuzumab. Additionally, the confocal microscopy images with FITC-labelled proteins clearly shows that trastuzumab interacts primarily with the cell membrane (Figure 26), while cetuximab is readily internalized into the cells (Figure 27). This can also be seen from the confocal microscopy images where the secondary antibody was used, although the difference was not as clear in these images as with the FITC-labelled proteins.

The accumulation of cetuximab into the cells is also indicated by the fact that the MP-SPR signal responses at the end of the 20-minute measurements increases and stays above the baseline, and that this increase is concentration dependent (Figure 20). The MP-SPR signal

response for IgG is also positive (Figure 21), which indicates that IgG induces a spreading of the cells in a similar manner as cetuximab. This is also seen from the confocal microscopy images where the cell nuclei in the case of IgG is of similar size as the cell nuclei for cetuximab and clearly larger compared to trastuzumab (Figures 26 and 28). However, the confocal microscopy images with FITC labelling shows that IgG do neither interact with the cell membrane nor is readily internalized by the cells (Figure 28), even though the MP-SPR signal response at the highest IgG concentration indicates that there might be some IgG internalized by the cells. This is, because the MP-SPR signal response stays on a higher level compared to the baseline at the end of the measurement. This demonstrates the difficulty to separate what interactions are measured simply from the MP-SPR signal response and often it is necessary to use complementary techniques such as confocal microscopy to clarify this. On the other hand, the confocal microscopy images taken with the secondary antibody suggests that some IgG actually are taken up by the cells (Figure 28), which would support that the MP-SPR signal response for IgG is also partly originating from cell uptake of IgG.

Concerning the long MP-SPR measurements there are difficulties to draw any conclusions from them. The variability of the measurements was probably due to many reasons. The most obvious reason was the formation of air bubbles in the tubing and flow channel during the measurements. Other reasons causing the variability in the measurements could the use of a wrong type of flow channel with dimensions that were not suitable for cell measurements, or the choice of the cell type could have been wrong, or the cell culturing protocol for seeding the cells on the sensor was not optimal. However, during this thesis work there was no time to try to optimize these. Thus, it is suggested that these issues must first be clarified, solved, and optimized before any new attempts for long MP-SPR measurements are planned or executed.

The LigandTracer measurements revealed that the original signal response was highest for trastuzumab, second highest for cetuximab and lowest for IgG (Figures 23-25). This suggests that trastuzumab and cetuximab interact readily with SK-OV-3 cells, while IgG do not considerably interact with the cells. The higher affinity towards the cells for trastuzumab in the LigandTracer measurements compared to cetuximab could reflect that trastuzumab primarily interacts with the receptors on the cell membrane and is not readily internalized. This, because if most of the sample is on the surface of the cells, then the fluorescence

intensity is higher and there should be a higher LigandTracer signal response compared to a situation where the sample is internalized into the cells, which can lead to a decrease in the fluorescence intensity and consequently a lower LigandTracer signal response. This type of interpretation of the LigandTracer results are supported by the MP-SPR and confocal microscopy results and would also cross-validate the MP-SPR and confocal microscopy results.

The affinities of the proteins towards the SK-OV-3 cells were determined to be 1.6 x 10^{-10} M for trastuzumab and 1,4 x 10^{-9} M for cetuximab. That correlates well with the theory that trastuzumab has a stronger affinity towards SK-OV-3 cells as the lower value indicates a stronger affinity.

The slight differences seen in the confocal microscopy images taken with FITC labelled proteins and by using the secondary antibody (AlexaFluor) could be due to that direct labeling of the proteins with FITC slightly influences the properties of the proteins, and consequently affects their interaction with the cells. Therefore, the use of secondary antibody in confocal microscopy would better resemble the experimental conditions in MP-SPR. There is a slightly better correlation between the MP-SPR results (Figures 19-21) and confocal microscopy results with the secondary antibody than with confocal microscopy results with FITC labelled proteins (Figures 26-28). Especially, in the case of IgG for which MP-SPR indicates some uptake by cells, which is also seen in the confocal microscopy images with the secondary antibody, but not in the confocal microscopy images with FITC labelled proteins. Nevertheless, both confocal microscopy imaging approaches still showed the same trend for the interaction of the proteins with the SK-OV-3 cells, i.e., trastuzumab interacts primarily with the cell membrane, cetuximab is readily internalized into cells, and IgG interacts very weekly with the cells and is hardly taken up by the cells.

7. CONCLUSIONS

The cell culturing process for SK-OV-3 cells and their seeding on MP-SPR sensor substrates were successfully performed. The mycoplasma sample was taken in the beginning of starting culturing SK-OV-3 cells, and microscopy pictures were continuously taken to guarantee the wellbeing of the cells. No signs of cell destruction were identified during the whole project.

The MP-SPR measurements did not give reliable results because of several problems with the instrument. The time planned to accomplish the project was not long enough to figure out the main reasons to the problems. It stays unclear whether the instrument can be used to distinguish between the surface interaction and the cell internalization of the proteins studied. However, some of the MP-SPR measurements performed for shorter times could be used to compare to the results obtained by confocal microscopy and LigandTracer.

The LigandTracer measurements gave reliable results when compared to the confocal microscopy images. The LigandTracer technique seem to be a suitable instrument to study the interactions between the SK-OV-3 cells and the proteins used in this project. The confocal microscopy images were taken successfully with two different fluorescence substances, which both led to almost similar results.

8. SUMMARY IN SWEDISH – SAMMANFATTNING PÅ SVENSKA

VÄXELVERKAN OCH CELLUPPTAGNINGSPROCESS AV BIOLOGISKA LÄKEMEDEL FÖR CANCER

8.1. Introduktion till projektet

Detta projekt är ett samarbete mellan Orion Pharma och Åbo Akademi. Orion Pharma står för allt material som behövdes i laboratoriearbetet. I projektet mättes interaktioner och växelverkan mellan EGFR- och HER_2-målinriktade biologiska antikroppar och humana adenokarsinomceller (SK-OV-3). Interaktionerna mellan antikropparna och cellerna studerades främst med tekniken ytplasmonresonans (SPR). Med denna teknik kan cellinteraktionerna mätas i realtid utan markörsubstanser, såsom fluorescerande ämnen.

Syftet med projektet var:

1. Att odla cellkulturer som innehåller SK-OV-3-äggstockscancerceller som överuttrycker både EGFR- och HER_2-receptorer, samt att studera hur de biologiska proteinbaserade läkemedel trastuzumab (HER_2-hämmare) och cetuximab (EGFR-hämmare) respektive den negativa kontrollen (IgG-protein) växelverkar med dessa celler.

2. Att använda ytplasmonresonanstekniken (SPR) för att mäta och registrera dessa interaktioner i realtid. Baserat på de uppmätta signalerna kan ytplasmonresonanstekniken övervägas för att skilja mellan ytinteraktionen och internaliseringen av de biologiska proven och cellerna.

3. Konfokalmikroskopi och LigandTracer teknikerna användes som kompletterade tekniker för att verifiera resultaten av SPR-mätningarna.

8.2. SPR-, LigandTracer- och konfokalmikroskopiteknikerna

Ytplasmonresonanstekniken (SPR) baserar sig på en optisk biosensor som kan mäta skillnader i kinetiken hos olika typer av makromolekylära interaktioner, samt små molekylära interaktioner med både låg och hög affinitet. Denna teknik har nyligen använts till exempel i applikationer inom mikrobiologi, virologi samt protein-, membran-, cell- och nukleinsyrainteraktionsmätningar (Pattnaik, 2005). I Finland har tekniken använts till exempel av Suutari et al. för markörfri övervakning av nanopartikelcellupptag och markörfri analys med flera parametrar för att separera G-proteinkopplade receptorsignalvägar (Suutari et al., 2016) (Suutari et al., 2020).

Ett exempel på ett SPR-reflektansspektra presenteras i figur 37A. Minimet i reflektansspektrumet ger information om vid vilken infallsvinkel ljuset absorberas av ytplasmoner (resonansvinkel). Positionen av minimet i SPR-kurvan skiftar beroende på förändringen i brytningsindex, som sker på grund av strukturella förändringar i molekylerna (såsom bindning) som ligger på sensorytan. Förändringen i resonansvinkeln sker beroende av mängden bundna molekyler från lösningen, med andra ord massökning. Ökningen av brytningsindex kan noteras genom en ökning av resonansvinkelns position. Dessa förändringar i SPR-svaret plottas med tiden i ett sensorgram. (Wong, 2020)

Ett SPR-sensorgram presenterar en kurva av förändringen i resonansvinkeln som funktion av tid. Ett exempel på ett SPR-sensorgram presenteras i figur 37b. SPR-sensogramet ger mycket information om mätningen, till exempel om bindningen mellan en ligand och målreceptorn, om bindningens specificitet, samt djupare information om kinetik, affinitet och koncentrationsskillnader av ämnet i fråga. Typiska faser av SPR-sensorgrammet är baslinje, association, steady-state, dissociation och regenerering, som också presenteras i Figur 37B (Wong, 2020).

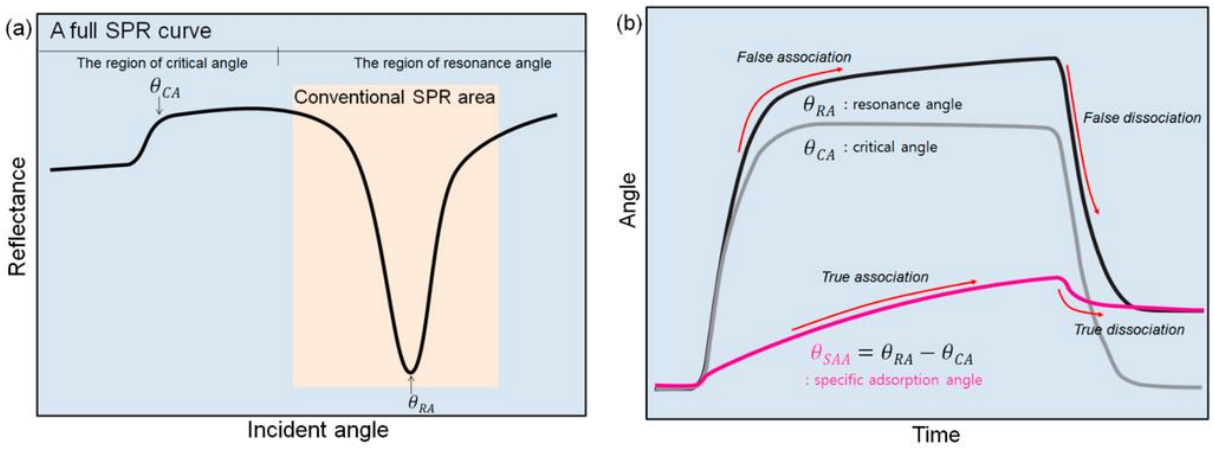

Figur 29. Ett exempel av a) ett SPR-kurva samt b) ett SPR-sensorgram (Wong, 2020).

LigandTracer-tekniken användes som en kompletterande teknik i det här projektet. Med denna teknik är det möjligt att särskilja affiniteten och kinetiken mellan liganden och receptorn (LigandTracer, 2023). Associations- och dissociationsfaserna mellan cellerna och liganderna mättes i realtid genom att använda fluorescerande substanser. En bild som förklarar principen av ett LigandTracer-instrument presenteras i Figur 30.

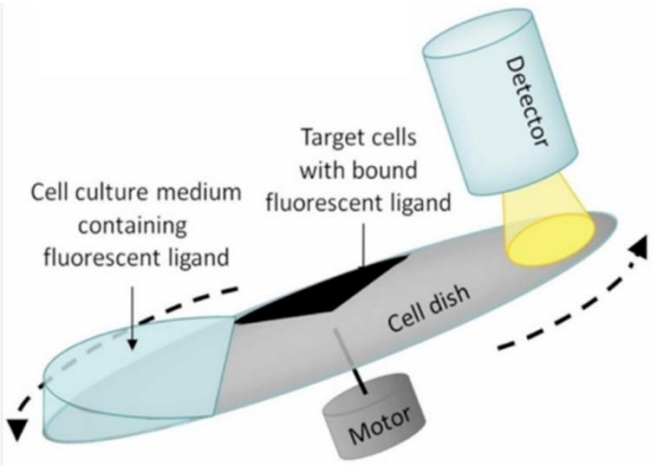

Figur 30. Principen av ett LigandTracer instrument (Umeå University, 2023).

Konfokalmikroskopi användes också som en kompletterande teknik i projektet för att verifiera resultaten från SPR-mätningarna. Metoden baserar sig på att producera en punktljuskälla som

genererar en komplett bild av provet genom att flytta fläcken över provet. Konfokalmikroskopi ger 3D-rekonstruktioner av proverna med hög upplösning och har en förmåga att avbilda djupt in i vävnaderna. (Elliott, 2020)

8.3. Proteinläkemedel och IgG

Immunoglobulin G (IgG) är den vanligaste immunoglobulinklassen hos människor. Molekylen består av två tunga kedjor, två lätta kedjor och Fc-regionen (Nezlin, 1998). Den primära funktionen av IgG hos människor är att binda till antigener från Fab-regionen (Painter, 1998). IgG kan också binda till Fc-receptorer på målceller, till exempel makrofager (Nezlin, 1998). Genom att binda till cellreceptorer av flera olika celltyper kan IgG bidra till fagocytos-processen, påverka den övergripande antikroppssyntesen och resultera i den antikroppsberoende cellulära cytotoxiciteten (ADCC) (Painter, 1998). IgG1-underklassen används i stor utsträckning för att utveckla olika terapeutiska antikroppar (Thomson, 2016). Strukturen för igG-molekylen presenteras i Figur 31.

IgG används som negativ kontroll i detta projekt. IgG-molekyler kan användas som kontroll för att avslöja eventuella icke-specifika bakgrundssignaler som kan störa signalerna av de studerade monoklonala antikropparna. Bakgrundssignaler av primära antikroppar kan orsakas till exempel genom bindningen till Fc-receptorer på målcellerna.

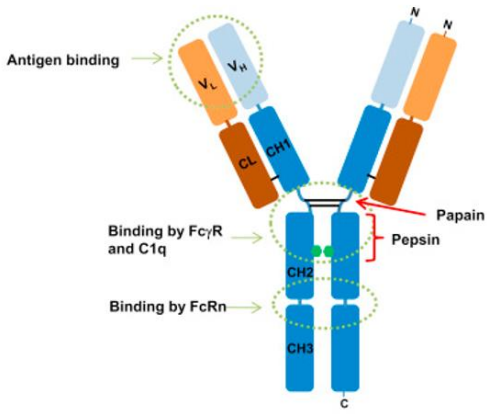

Figur 31. Strukturen av IgG-molekylen (Thomson, 2016).

Trastuzumab är en humaniserad monoklonal antikropp som binder till den humana epidermala tillväxtfaktor-receptorn ($EGFR_2$), även känd som HER_2-receptorn (Drugbank a), 2023). De monoklonala antikropparna är proteiner som har hög specificitet och affinitet för molekylen de har genererats mot. Trastuzumab har genererats genom att implantera ursprungligt murina proteinslingor till humana immunglobuliner (Malik och Ghatol, 2023).

Trastuzumab binder selektivt med en hög affinitet till den extracellulära domänen av HER_2-proteinet (Trastuzumab, Drugbank, 2023). Det har också anti-humana antikroppsegenskaper, inklusive bindning till de primära antikropparna. Det kan till exempel hjälpa till med detektion och sortering av målantigenerna genom att förbättra signalen som leder till högre känslighet och selektivitet. (AAT Bioquest, 2021; Drugbank a), 2023)

Trastuzumab används i stor utsträckning i behandlingen av metastaserande bröstcancer som utrycker den humana epidermala tillväxtfaktorreceptorn (HER_2), till exempel för dem som har ett överuttryck av HER_2-proteinet i tumörerna. Så mycket som cirka 20–30 % av bröstcancerfallen beräknas uppstå från den onormala aktiviteten eller överuttrycket av HER_2. Aktiveringen av HER_2 i cancerceller utlöser flera olika nedströmsvägar, vilket kan leda till en onormal proliferation av cellerna. Tillväxt och proliferation av cancerceller kan direkt och indirekt påverkas av och undertryckas med trastuzumab. (Trastuzumab, Drugbank, 2023). Trastuzumab kan också underlätta den antikroppsberoende cellulära cytotoxiciteten (ADCC), där effektorcellerna känner igen de antikroppsbelagda cellerna, vilket leder till cancercellens död (Gómez Román et al., 2014) Greenblatt och Khaddour, 2023). Trastuzumab används också för att behandla metastaserad bröstcancer i kombination med andra behandlingsmetoder och för att behandla metastaserande magcancer (EMA, 2018).

Cetuximab är en rekombinant chimär monoklonal antikropp (mAb) som binder konkurrenskraftigt till epidermal tillväxtfaktorreceptor (EGFR) (Drugbank b), 2023). Bindning av cetuximab till en epidermal tillväxtfaktorreceptor hämmar kompetitivt bindningen av epidermal tillväxtfaktor (EGF) till receptorn (Drugbank b), 2023). Vanligtvis styr bindningen av EGF till EGFR tillväxten av celler och inducerar cellsignaleringsvägarna som leder till celldelning. I cancerceller kan en muterad och överuttryckt EGFR göra att cancercellerna delar sig okontrollerat. (NCI, 2011). Inhiberingen av EGFR-signalvägarna leder till nedreglering av cellcykelprogression och cellöverlevnad. Bindningen av cetuximab till EGFR inducerar också

cellapoptos (celldöd) och hämmar produktionen av celltillväxtfaktorerna, samt främjar den antikroppsberoende cellulära cytotoxiciteten, såsom trastuzumab. (Drugbank b), 2023)

Cetuximab används för att behandla metastaserade EGFR-involverad metastaserade tjocktarms- och ändtarmscancer, som innebär icke-muterade versioner av RAS-genfamiljen. Det kan användas som en enda behandling eller tillsammans med andra behandlingar beroende på cancertypen. Det kan också användas för att behandla skivepitelcancer i huvud och nacke (såsom mun, svalg eller struphuvud), vanligtvis som en kombinationsbehandling med till exempel strålbehandling.

8.4. Resultat och diskussion

Resultaten från SPR-mätningarna med 20 minuters injektionstid presenteras i Figur 32. Trastuzumab gav negativa SPR responser speciellt i början av injektionerna, medan cetuximab gav positiva SPR responser. Resultaten tycks vara koncentrationsberoende, eftersom de högre koncentrationerna gav högre respons än de lägre koncentrationerna. Resultaten från IgG-mätningarna var inte helt reproducerbara, eftersom två olika mätningar med en koncentration av 6nM gav helt olika resultat. Längre mätningar (4 timmar) gav inga pålitliga resultat, utan alla diagram såg olika ut oberoende av proteinet eller dess koncentration.

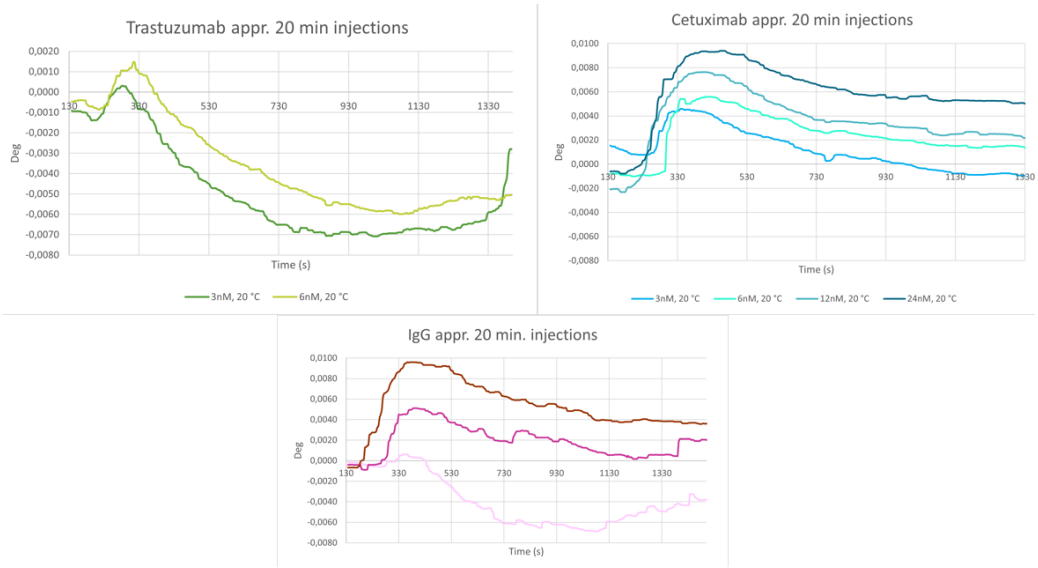

Figur 32. SPR-mätningarna av trastuzumab, cetuximab och igG (12nM), med 20 minuters injektioner (Osmonen, 2023).

LigandTracer-mätningarna stöder resultaten från konfokalmikroskopin genom att trastuzumab hade den högsta responsen, cetuximab hade en måttlig respons och igG endast hade en svag respons.

I Figur 33 presenteras konfokalmikroskopibilderna av alla proteiner. Där syns det tydligt hur de forskade proteinläkemedlen och IgG växelverkar med SK-OV-3-cellerna. Trastuzumab ackumuleras speciellt mycket till cellytan, då cetuximab växelverkar måttligt med cellytan, och en del av molekylerna tas upp i cellerna. IgG växelverkar ytterst svagt med cellerna.

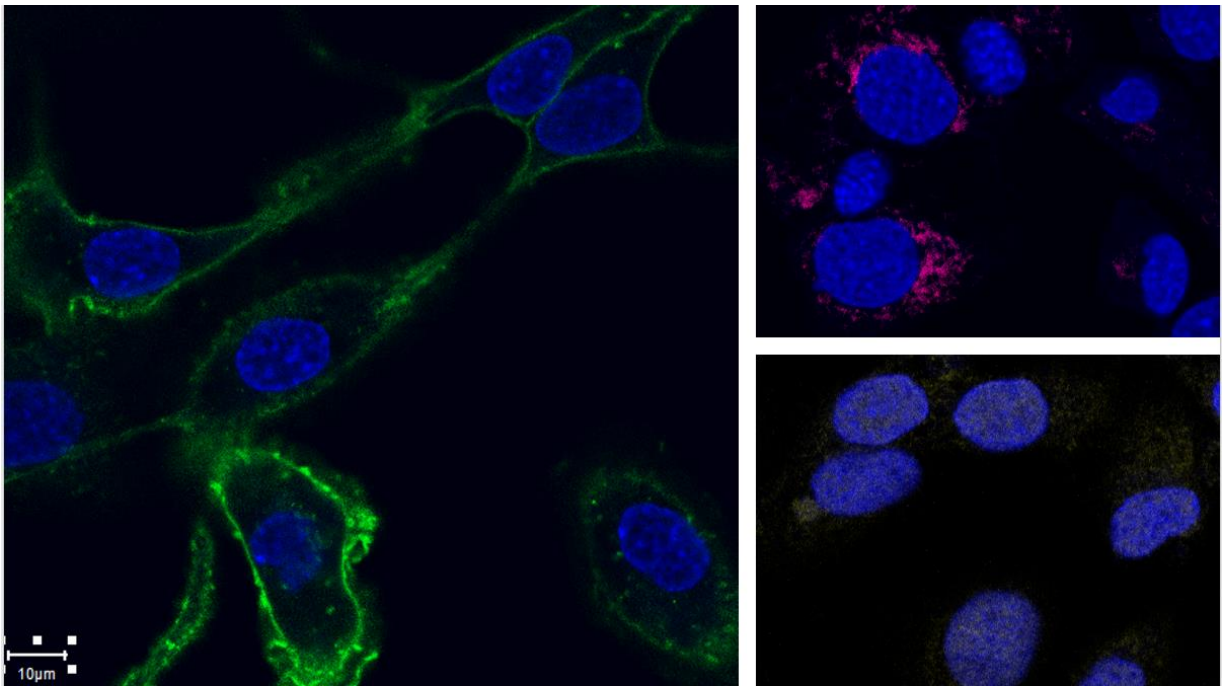

Figur 33. En konfokalmikroskopibild av trastuzumab och cellerna (trastuzumab som grön, cellkärnan alltid som blå), cetuximab och cellerna (cetuximab som ljusröd) och IgG och cellerna (IgG som gul) (Osmonen, 2023).

9. REFERENCES

AAT Bioquest, 2021. AAT Bioquest [WWW Document]. URL https://www.aatbio.com/resources/faq-frequently-asked-questions/What-do-anti-human-antibodies-bind-to (accessed 3.28.23).

ATCC, 30-2007, 2022. McCoy's 5A Medium - 30-2007 | ATCC [WWW Document]. URL https://www.atcc.org/products/30-2007 (accessed 3.21.23).

Biolabs, 2017. Creative Biolabs Blog. URL https://www.creative-biolabs.com/blog/index.php/recombinant-antibody/ (accessed 3.28.23).

Bionavis, 2021. Sensor slides | BioNavis MP-SPR measuring equipments [WWW Document]. URL https://www.bionavis.com/en/products/additional-options-and-consumables/sensor-slides/ (accessed 4.6.23).

bitesizebio, 2017. Explained: Sensor Chips for Surface Plasmon Resonance and Other Applications [WWW Document]. URL https://bitesizebio.com/34644/biosensor-chips-surface-plasmon-resonance/ (accessed 4.4.23).

CreativeBiomart, 2023. Principle and Protocol of Surface Plasmon Resonance (SPR) - Creative BioMart [WWW Document]. URL https://www.creativebiomart.net/resource/principle-protocol-principle-and-protocol-of-surface-plasmon-resonance-spr-361.htm (accessed 4.4.23).

Drugbank a), 2023. Trastuzumab, Drugbank [WWW Document]. URL https://go.drugbank.com/drugs/DB00072 (accessed 3.23.23).

Drugbank b), 2023. Cetuximab, Drugbank [WWW Document]. URL https://go.drugbank.com/drugs/DB00002 (accessed 3.23.23).

Elliott, A.D., 2020. Confocal Microscopy: Principles and Modern Practices. Curr Protoc Cytom 92, e68. https://doi.org/10.1002/cpcy.68

EMA, 2018. Herceptin [WWW Document]. European Medicines Agency. URL https://www.ema.europa.eu/en/medicines/human/EPAR/herceptin (accessed 3.28.23).

Gómez Román, V.R., Murray, J.C., Weiner, L.M., 2014. Chapter 1 - Antibody-Dependent Cellular Cytotoxicity (ADCC), in: Ackerman, M.E., Nimmerjahn, F. (Eds.), Antibody Fc. Academic Press, Boston, pp. 1–27. https://doi.org/10.1016/B978-0-12-394802-1.00001-7

Greenblatt, K., Khaddour, K., 2023. Trastuzumab, in: StatPearls. StatPearls Publishing, Treasure Island (FL).

Griffin, G.D., Stratis-Cullum, D.N., McKnight, T.E., 2019. Biosensors☆, in: Schmidt, T.M. (Ed.), Encyclopedia of Microbiology (Fourth Edition). Academic Press, Oxford, pp. 542–574. https://doi.org/10.1016/B978-0-12-801238-3.02488-0

Gunturu, K.S., Woo, Y., Beaubier, N., Remotti, H.E., Saif, M.W., 2013. Gastric cancer and trastuzumab: first biologic therapy in gastric cancer. Ther Adv Med Oncol 5, 143–151. https://doi.org/10.1177/1758834012469429

Jang, D., Chae, G., Shin, S., 2015. Analysis of Surface Plasmon Resonance Curves with a Novel Sigmoid-Asymmetric Fitting Algorithm. Sensors 15, 25385–25398. https://doi.org/10.3390/s151025385

LigandTracer, 2023. LigandTracer – Real-time interaction measurements on live cells. URL https://www.ligandtracer.com/ (accessed 3.28.23).

lino-Biotech, 2021. Surface Plasmon Resonance (SPR). lino Biotech AG. URL https://www.lino-biotech.com/surface-plasmon-resonance-spr/ (accessed 4.4.23).

Malik, B., Ghatol, A., 2023. Understanding How Monoclonal Antibodies Work, in: StatPearls. StatPearls Publishing, Treasure Island (FL).

Masson, J.-F., Banerji, S., Kim, Y.-C., Booksh, K., 2004. Surface plasmon resonance sensors for industrial applications. Proceedings of SPIE - The International Society for Optical Engineering 5586. https://doi.org/10.1117/12.580124

NCI, 2011. Definition of EGFR - NCI [WWW Document]. URL https://www.cancer.gov/publications/dictionaries/cancer-terms/def/egfr (accessed 3.29.23).

Nezlin, R., 1998. CHAPTER 1 - General Characteristics of Immunoglobulin Molecules, in: Nezlin, R. (Ed.), The Immunoglobulins. Academic Press, New York, pp. 3–73. https://doi.org/10.1016/B978-012517970-6/50001-1

Nguyen, H.H., Park, J., Kang, S., Kim, M., 2015. Surface Plasmon Resonance: A Versatile Technique for Biosensor Applications. Sensors (Basel) 15, 10481–10510. https://doi.org/10.3390/s150510481

Olympus Lifescience, n.d. Confocal Microscopy - Introduction | Olympus LS [WWW Document]. URL https://www.olympus-lifescience.com/en/microscope-resource/primer/techniques/confocal/confocalintro/ (accessed 4.6.23).

Osmonen, 2023. Picture.

Painter, R.H., 1998. IgG, in: Delves, P.J. (Ed.), Encyclopedia of Immunology (Second Edition). Elsevier, Oxford, pp. 1208–1211. https://doi.org/10.1006/rwei.1999.0313

Pattnaik, P., 2005. Surface plasmon resonance. Appl Biochem Biotechnol 126, 79–92. https://doi.org/10.1385/ABAB:126:2:079

Proteintech, 2022. IF imaging: Widefield versus confocal microscopy [WWW Document]. URL https://www.ptglab.com/news/blog/if-imaging-widefield-versus-confocal-microscopy/ (accessed 4.6.23).

Puiu, M., Bala, C., 2016. SPR and SPR Imaging: Recent Trends in Developing Nanodevices for Detection and Real-Time Monitoring of Biomolecular Events. Sensors (Basel) 16, 870. https://doi.org/10.3390/s16060870

ResearchGate, 2008. Structure of Cetuximab [WWW Document]. ResearchGate. URL https://www.researchgate.net/figure/Structure-of-Cetuximab_fig2_5513931 (accessed 3.28.23).

SKOV3 ATCC, 2022. SK-OV-3-HTB-77 | ATCC [WWW Document]. URL https://www.atcc.org/products/htb-77 (accessed 3.21.23).

SPR-Pages, 2022. SPRpages Home [WWW Document]. URL https://sprpages.nl/ (accessed 4.1.23).

Stenberg, J., Spiegelberg, D., Karlsson, H., Nestor, M., 2013. Choice of labeling and cell line influences interactions between the Fab fragment AbD15179 and its target antigen CD44v6. Nuclear medicine and biology 41. https://doi.org/10.1016/j.nucmedbio.2013.10.010

Suutari, T., Rahman, S.N., Vischer, H.F., van Iperen, D., Merivaara, A., Yliperttula, M., Leurs, R., Kool, J., Viitala, T., 2020. Label-Free Analysis with Multiple Parameters Separates G Protein-Coupled Receptor Signaling Pathways. Anal. Chem. 92, 14509–14516. https://doi.org/10.1021/acs.analchem.0c02652

Suutari, T., Silen, T., S¸en Karaman, D., Saari, H., Desai, D., Kerkelä, E., Laitinen, S., Hanzlikova, M., Rosenholm, J.M., Yliperttula, M., Viitala, T., 2016. Real-Time Label-Free Monitoring of Nanoparticle Cell Uptake. Small 12, 6289–6300. https://doi.org/10.1002/smll.201601815

The emerging sciences, 2022. Types of Water: Mili-Q water, ELIX water, and Distilled water | 2022 [WWW Document]. URL https://theemergingsciences.com/types-of-water/ (accessed 4.14.23).

ThermoFisher, a), 2023. Thawing Frozen Cells [WWW Document]. URL https://www.thermofisher.com/uk/en/home/references/gibco-cell-culture-basics/cell-culture-protocols/thawing-cells.html (accessed 3.22.23).

ThermoFisher b), 2023. Cell Culture Media Supplements - FI [WWW Document]. URL https://www.thermofisher.com/uk/en/home/life-science/cell-culture/mammalian-cell-culture/media-supplements.html (accessed 3.29.23).

ThermoFisher c), 2023. Human IgG Isotype Control (31154) [WWW Document]. URL https://www.thermofisher.com/antibody/product/Human-IgG-Isotype-Control/31154 (accessed 3.30.23).

Thomson, C.A., 2016. IgG Structure and Function, in: Ratcliffe, M.J.H. (Ed.), Encyclopedia of Immunobiology. Academic Press, Oxford, pp. 15–22. https://doi.org/10.1016/B978-0-12-374279-7.05002-5

Umeå University, 2023. LigandTracer® Green [WWW Document]. URL https://www.umu.se/en/research/infrastructure/biochemical-imaging-centre-umea-bicu/ligand-tracer/ (accessed 4.5.23).

Viitala et.al., 2013. Elucidating the Signal Responses of Multi-Parametric Surface Plasmon Resonance Living Cell Sensing: A Comparison between Optical Modeling and Drug–MDCKII Cell Interaction Measurements | PLOS ONE [WWW Document]. URL https://journals.plos.org/plosone/article?id=10.1371/journal.pone.0072192 (accessed 5.6.23).

Warwick University, 2017. University of Warwick Business Facilities - Analytical Equipment - Confocal Microscopy [WWW Document]. URL https://warwick.ac.uk/services/ris/impactinnovation/impact/analyticalguide/confocal/ (accessed 4.6.23).

Wong, A., 2020. SPR Sensorgram Explained [WWW Document]. Affinite Instruments. URL https://www.affiniteinstruments.com/post/spr-sensorgram-explained (accessed 4.4.23).

APPENDIX

Appendix 1.

Thawing frozen cells

1. Remove the cryovial containing the frozen cells from liquid nitrogen storage and immediately place it into a 37 °C water bath.
2. Quickly thaw the cells (< 1 minute) by gently swirling the vial in the 37 °C water bath until there is just a small bit of ice left in the vial.
3. Transfer the vial into a laminar flow hood (Thermo Scientific biological safety cabinet). Before opening, wipe the outside of the vial with 70% ethanol.
4. Transfer the desired amount of pre-warmed complete growth medium dropwise into the centrifuge tube containing the thawed cells.
5. Centrifuge the cell suspension at approximately 200 × g for appr. 8 minutes (in Eppendorf Centrifuge 5702). The actual centrifugation speed and duration varies depending on the cell type.
6. After the centrifugation, check the clarity of supernatant and visibility of a complete pellet. Aseptically decant the supernatant without disturbing the cell pellet.
7. Gently resuspend the cells in complete growth medium and transfer them into the cell culture plate and into the incubator (Eppendorf CellXpert).

Appendix 2.

Subculturing procedure protocol for the SK-OV-3 cells (using the 100x20mm plate)

The instructions were received from Åbo Akademi University's cell laboratory, and modified according to the information of the SK-OV-3 cell line on the ATCC website (SKOV3 ATCC, 2022)

1. Remove and discard the culture medium in the Thermo Scientific biological safety cabinet. Wash with warm PBS solution (2.0 to 3.0 ml, 37 °C).
2. Briefly rinse the cell layer with PBS solution to remove all traces of serum that contains trypsin inhibitor. Remove the PBS solution with a laboratory vacuum pump.
3. Add 2.0 to 3.0 ml trypsin-EDTA solution to the plate and observe the cells under an inverted microscope (Nikon TMS instrulab) until the cell layer is dispersed (usually within 5 minutes). Note: Shaking the flask with the cells while waiting for the cells to detach is not recommended because of the risk of clumping. The cell plate may be placed at 37 °C Eppendorf CellXpert incubator to facilitate the dispersal.
4. Add 4.0 to 5.0 ml of complete growth medium and aspirate the cells by gently pipetting.
5. Transfer the cells to a 15 ml falcon tube and centrifuge them at 200 x g for 3 minutes (Eppendorf Centrifuge 5702).
6. Resuspend the cell pellet in a minimal volume (4.0 ml) of the pre-warmed complete growth medium (and remove a sample for counting).
7. (Determine the total number of cells)
8. Dilute the cell suspension to the seeding density and pipet an appropriate volume (10 ml) into new cell culture plates and turn the cells to the incubator at 37 °C (Eppendorf CellXpert).

Appendix 3.

Instructions for LigandTracer

The instructions were received from Åbo Akademi University's laboratory personal.

1. Culture the cells on a fibronectin coated plate until the number of cells reaches appr. 1 million.
2. Put the cell plate into the instrument without lock.
3. Start the measurement and continue until a stable baseline is reached. That should happen in 15-20 minutes.
4. The sample can be injected when the baseline has been reached. The instrument should be paused when the sample is pipetted onto the plate.
5. The measurement will continue until the preferred time has passed.